

**T.R.**  
**GEBZE TECHNICAL UNIVERSITY**  
**GRADUATE SCHOOL OF NATURAL AND APPLIED SCIENCES**

**EVALUATION OF  $CPT_u$  – SPT CORRELATIONS FOR  
TRANSITIONAL SOILS**

**MUSTAFA HABİBOĞLU**  
**A THESIS SUBMITTED FOR THE DEGREE OF**  
**MASTER OF SCIENCE**  
**DEPARTMENT OF CIVIL ENGINEERING**

**GEBZE**  
**2022**

**T.C.**  
**GEBZE TEKNİK ÜNİVERSİTESİ**  
**FEN BİLİMLERİ ENSTİTÜSÜ**

**GEÇİŞ ZEMİNLERİ İÇİN CPT<sub>u</sub> - SPT**  
**KORELASYONLARININ**  
**DEĞERLENDİRİLMESİ**

**MUSTAFA HABİBOĞLU**  
**YÜKSEK LİSANS TEZİ**  
**İNŞAAT MÜHENDİSLİĞİ ANABİLİM DALI**

**DANIŞMANI**  
**DOC. DR. ABDULLAH TOLGA ÖZER**

**GEBZE**  
**2022**

**T.R.**  
**GEBZE TECHNICAL UNIVERSITY**  
**GRADUATE SCHOOL OF NATURAL AND APPLIED SCIENCES**

**EVALUATION OF CPT<sub>u</sub> AND SPT  
CORRELATIONS FOR TRANSITIONAL  
SOILS**

**MUSTAFA HABİBOĞLU**  
**A THESIS SUBMITTED FOR THE DEGREE OF  
MASTER OF SCIENCE  
DEPARTMENT OF CIVIL ENGINEERING**

**THESIS SUPERVISOR**  
**ASSOC. PROF. DR. ABDULLAH TOLGA ÖZER**

**GEBZE**  
**2022**

<b>GEBZE TEKNİK ÜNİVERSİTESİ</b>	<b>YÜKSEK LİSANS JÜRİ ONAY FORMU</b>
----------------------------------	--------------------------------------

GTÜ Fen Bilimleri Enstitüsü Yönetim Kurulu'nun 30/06/2022 tarih ve 2022/33 sayılı kararıyla oluşturulan jüri tarafından 21/07/2022 tarihinde tez savunma sınavı yapılan Mustafa HABİBOĞLU'nun tez çalışması İnşaat Mühendisliği Anabilim Dalında YÜKSEK LİSANS tezi olarak kabul edilmiştir.

### **JÜRİ**

ÜYE

(TEZ DANIŞMANI) : Doç. Dr. Abdullah Tolga Özer

ÜYE

: Prof. Dr. Selçuk Toprak

ÜYE

: Doç. Dr. Mustafa Kubilay KELEŞOĞLU

### **ONAY**

Gebze Teknik Üniversitesi Fen Bilimleri Enstitüsü Yönetim Kurulu'nun  
...../...../..... tarih ve ...../..... sayılı kararı.

İMZA/MÜHÜR

## SUMMARY

The standard penetration test, SPT, is one of the most used tests to characterize the subsurface profile. Despite its widespread use, there are still various issues regarding the repeatability of the SPT results. The normalized SPT blow count is used to estimate the physical and mechanical properties of the soil and used in the foundation design. The piezocone test, CPTu, is used to characterize the in-situ soil properties. CPTu provides continuous data recording along the subsurface profile and the repeatability is more reliable comparing to that of SPT. On the other hand, disturbed soil samples can be collected by SPT.

The extensive SPT testing program carried out by the Northern Marmara Highway, KMO, project for subsurface soil characterization along the Section 6 of the project between Km 223 and Km 251 where subsurface profile consists of transitional soils such as clayey silts, silty clays and silts. In addition to SPT tests, CPTu testing program was also performed to characterize the in-situ properties along the Section 6 of the highway route. The results of these CPTu tests and SPT tests was used as a case study. Comprehensive correlation of these two in-situ soil characterization test methods was studied.

A historical review of the existing literature on estimating SPT blow counts using CPTu test results was evaluated. Evaluation of the effectiveness of CPTu to predict the SPT blow counts of transitional soils was accomplished by comparing the CPTu test results and SPT results. New equations are proposed to improve existing equations.

**Key Words: Standard penetration test (SPT), piezocone test (CPTu), Northern Marmara Highway (KMO).**

## ÖZET

Standart penetrasyon testi, SPT, geoteknik arazi karakterizasyonunda yaygınlıkla kullanılan deneylerden biridir. Yaygın kullanımına rağmen, SPT sonuçlarının tekrar edilebilirliği ile ilgili hala çeşitli sorunlar bulunmaktadır. Normalize edilmiş SPT vuruş sayısı, zeminin fiziksel ve mekanik özelliklerini tahmin etmek amacıyla ve temel tasarımında kullanılır. Piezocone testi, CPTu, arazide zemin özelliklerini karakterize etmek için kullanılan bir diğer metottür. CPTu, yeraltı profili boyunca sürekli veri kaydı sağlar ve tekrar edilebilirliği SPT'ye kıyasla daha yüksektir. Öte yandan, örselenmiş zemin numuneleri SPT ile toplanabilir. Bu nedenle, sahanın idealize edilmiş zemin profilini oluşturmak için geoteknik saha inceleme projelerinde hem SPT hem de CPTu birlikte kullanılır.

Kuzey Marmara Otoyolu (KMO) tarafından Km 223 ile Km 251 arasında kalan 6. Bölümü boyunca yürütülen kapsamlı SPT deney programı neticesinde, zemin profilinin killi siltler, siltli killer ve siltler gibi geçiş zeminlerinden (transient soil) oluştuğu tespit edilmiştir. SPT deneylerine ek olarak, karayolu güzergahının 6. Bölümü boyunca arazide özelliklerini karakterize etmek için CPTu deney programı da gerçekleştirilmiştir. Bu CPTu ve SPT sonuçları bir vaka çalışması olarak kullanılmıştır. Bu iki arazi deneyinin arazi karakterizasyonu yöntemlerinin kapsamlı korelasyonu incelenmiştir.

CPTu test sonuçlarını kullanarak SPT vuruş sayılarını tahmin etmeye ilişkin mevcut literatürün incelemesi yapılmıştır. CPTu'nun geçiş zeminlerinin (transient soils) SPT vuruş sayılarını tahmini, CPTu test sonuçları ve SPT sonuçları karşılaştırılarak gerçekleştirilmiştir. Mevcut denklemlerin tahmin performansını iyileştirmek için ek regresyon analizleri yapılarak ve geçiş zeminleri için denklemler önerilmiştir. Önerilen korelasyonlar, KMO'nun 6. Bölümü boyunca inşa edilecek gelecekteki altyapı gelişmeleri için bir kılavuz olarak kullanılabilir.

**Anahtar Kelimeler: Standart penetration testi (SPT), piezocone testi (CPTu), Kuzey Marmara Otoyolu (KMO).**

## ACKNOWLEDGEMENTS

I would like to express my deep and sincere gratitude to my supervisor, Associate Professor Abdullah Tolga ÖZER, who not only shared his profound scientific knowledge with me but also taught me great lessons of life. His support, suggestions and encouragement gave me the drive and will to complete this work.

I wish to express my warm and sincere thanks to the Northern Marmara Highway, KMO, ANADOLU OTOYOLU İŞLETME A.Ş for their collaboration to this research. I appreciate the support of İlyas Bulut, General Manager of the KMO, Ayhan Arda, Construction Manager of the KMO and İsmail Naiboğlu, Geotechnical Works Manager of the KMO.

I am grateful to my friends Defne BARIŞ and Burak KARAOĞLU for their support.

Finally, I would like to thank my dear parents for their unconditional support and love throughout my education life.

# TABLE of CONTENTS

	<b><u>Page</u></b>
SUMMARY	v
ÖZET	vi
ACKNOWLEDGMENTS	vii
TABLE of CONTENTS	viii
LIST of ABBREVIATIONS and ACRONYMS	x
LIST of FIGURES	xiii
LIST of TABLES	xvi
1. INTRODUCTION	1
2. SPT-CPT CORRELATION	7
2.1. Standard Penetration Tests (SPT)	7
2.1.1. Experimental Procedure	7
2.1.2. Factors Affecting SPT Results and Corrections	9
2.2. Piezocone Tests (CPTu)	11
2.2.1. Types of CPT	13
2.2.2. Mechanical Cone Penetrometers	13
2.2.3. Electric Cone Penetrometers	14
2.2.4. Seismic CPT (SCPTu)	16
2.2.5. Data Obtained by CPTu	16
3. SOIL BEHAVIOUR TYPE	19
3.1. Non-Normalized SBT Charts	19
3.2. Normalized SBT (SBT <sub>n</sub> ) Charts	19
3.3. Transitional Soil	23
4. GEOLOGY of THE STUDY AREA	29
5. SPT and CPTu CORRELATIONS	34
6. EVALUATION of CPTu – SPT N DATABASE of SECTION 6 of THE KMO	40
6.1. Soil Behaviour Type	45
6.2. Predictive Performances of Previous Studies	48
6.3. Correlation of This Study	56

6.3.1. Predictive Performance of Proposed Equations	58
7. CONCLUSION	60
REFERENCES	76
BIOGRAPHY	61
APPENDICES	68
Other Appendices (CD)	68



## LIST of ABBREVIATIONS and ACRONYMS

<b><u>Abbreviations</u></b>	<b><u>Explanations</u></b>
<b><u>and Acronyms</u></b>	
$\Delta u$	: Excess pore pressure
$\sigma'_v$	: Effective vertical stress
$\sigma_{v0}$	: Vertical stress
$i$	: Dynamic porewater pressure gradient
$B_q$	: Normalized pore pressure parameter
$C_A$	: Casing head correction
$C_B$	: Borehole diameter correction
$C_{BF}$	: Hammer blow count frequency correction
$C_C$	: Hammer pad correction
cm	: Centimetre
$C_N$	: Overburden stress correction factor
$C_R$	: Rod length correction
$C_S$	: Sampling method
d	: Diameter
$D_{50}$	: Median grain size
$D_r$	: Relative density
$E_R$	: Hammer efficiency
$F_r$	: Normalized friction ratio
$f_s$	: Sleeve friction
$f_t$	: Corrected friction resistance
ft	: Feet
func	: function
$I_c$	: Soil behaviour type index
Inc	: Incorporated
kg	: Kilogram
kgf	: Kilograms-force
kPa	: Kilopascal
m	: Meter
min	: Minute

mm	:	Millimetre
MPa	:	Megapascal
N	:	Blow count of standard penetration test
N <sub>55</sub>	:	Corrected N value by 55 percent of theoretical free-fall hammer energy
N <sub>60</sub>	:	Corrected N value by 60 percent of theoretical free-fall hammer energy
(N <sub>1</sub> ) <sub>60</sub>	:	60% energy and overburden correction factor applied blow count
(N <sub>1</sub> ) <sub>60CS</sub>	:	SPT blow count corrected for overburden pressure, energy, and fines content
Pa	:	Atmospheric pressure (100 kPa)
psi	:	Pound per square inch
q <sub>c</sub>	:	Cone penetration tip resistance
q <sub>c1</sub>	:	Corrected cone penetration test tip resistance
q <sub>c1-CS</sub>	:	CPT tip resistance corrected for overburden pressure and fines content
q <sub>n</sub>	:	Net cone resistance
q <sub>t</sub>	:	Corrected tip resistance
Q <sub>t</sub>	:	Normalized cone resistance
R <sup>2</sup>	:	Regression
R <sub>f</sub>	:	Friction ratio
u	:	Porewater pressure
u <sub>2</sub>	:	Penetration pore pressure behind the cone tip
V <sub>s</sub>	:	Shear wave velocity
ASTM	:	American Society for Testing and Materials
CPT	:	Cone Penetration Test
CPTu	:	Piezometric Electric Cone Penetration Test, Piezocone Test
FC	:	Fines Content
FHWA	:	Federal Highway Administration
KMO	:	Northern Marmara Highway
N/A	:	Not assessed
PMT	:	Pressuremeter Test
SBT	:	Soil Behaviour Type
SBT <sub>n</sub>	:	Normalized Soil Behaviour Type

SCPTu : Seismic Piezometric Electric Cone Penetration Test  
SPT : Standard Penetration Test  
UK : United Kingdom  
USA : United States of America



## LIST of FIGURES

<b><u>Figure No:</u></b>	<b><u>Page</u></b>
1.1: Northern Marmara Motorway Route.	2
1.2: Yavuz Sultan Selim Bridge.	2
1.3: A viaduct at the region 6 of the KMO.	3
1.4: A bridge at the region 6 of the KMO.	3
1.5: A partial cloverleaf interchange at the region 6 of the KMO.	4
1.6: An overpass at the region 6 of the KMO.	4
1.7: A partial cloverleaf interchange with an underpass and hydraulic culvert at the region 6 of the KMO.	5
2.1: Performing the standard penetration test.	8
2.2: Standard penetration test steps.	8
2.3: CPT probes.	13
2.4: Mechanical cone.	14
2.5: Begemann type cone with friction sleeve.	14
2.6: Piezometric Electric CPT (CPTu).	15
2.7: Electric piezometric cone penetrometer.	15
2.8: Seismic CPT (SCPTu).	16
3.1: Non-normalized CPT Soil Behavior Type (SBT) chart.	20
3.2: Normalized CPT Soil Behavior Type (SBT) chart.	21
3.3: Normalized CPT Soil Behavior Type (SBTn) charts $Q_t - F_r$ and $Q_t - B_q$	22
3.4: Location of North Sea clay data of Ramsey (2002) superimposed on Robertson's (1990) chart.	24
3.5: Soil classification charts	25
3.6: Comparison of chart proposed by Schneider et al., 2008 with Robertson (1990).	26
3.7: Soil classification chart.	28
4.1: Morphology of the region.	30
4.2: North Anatolian Fault Line.	31
4.3: Geomorphology and geology of Adapazari.	31
4.4: Sakarya River.	32

4.5:	Generalized subsurface soil profiles in Adapazarı.	32
4.6:	Soil behaviour type of Adapazarı Region based on Schneider et al. (2008).	33
5.1	CPT-SPT correlations with mean grain size.	37
5.2	CPT-SPT correlation based on grain size.	38
5.3	CPT-SPT correlation based on fine content.	38
5.4	SPT-CPT correlations in terms of $(q_t/Pa)/N_{60}$ and CPT-based SBT index $I_c$ .	39
6.1:	A typical SPT boring log.	41
6.2:	A typical CPTu data report.	42
6.3:	Sections 87 through 90.	42
6.4:	Aerial view of the alignment and locations of SPT borings and CPTu soundings at the section 89.	43
6.5:	Aerial view of the alignment and locations of SPT borings and CPTu soundings at the section 87.	43
6.6:	A typical CPTu data versus elevation.	44
6.7:	A typical SPT data versus elevation.	45
6.8:	A typical SBT index versus elevations graph.	46
6.9:	KMO data based on Robertson (1990).	47
6.10:	KMO data based on Schneider et al. (2008).	47
6.11:	De Alencar Velloso (1959) equation versus CPTu data.	49
6.12:	Franki Piles (1960) from Akca (2003) equation versus CPTu data.	49
6.13:	Alam et al., (2018) equation versus CPTu data.	50
6.14:	Hore et al., (2018) equation versus CPTu data.	50
6.15:	Jarushi et al., (2015) equation versus CPTu data.	51
6.16:	Kara and Gündüz (2010) equation versus CPTu data.	51
6.17:	Shahri et al., (2014) equation versus CPTu data.	52
6.18:	Aral and Güneş (2017) equation versus CPTu data.	52
6.19:	Robertson (2012) equation versus CPTu data.	53
6.20:	Predictive performance of previous works on section 87.	54
6.21:	Predictive performance of previous works on section 89.	55
6.22:	SPT-N versus $q_c/Pa$ graph.	56
6.23:	SPT- $N_{60}$ versus $q_c/Pa$ graph.	56
6.24:	$q_t/Pa/N$ versus $I_c$ graph.	57

6.25: Predictive performance of the proposed equations for the sections 89.	58
6.26: Predictive performance of of the proposed equations for the section 87.	58



## LIST of TABLES

<b><u>Table No:</u></b>	<b><u>Page</u></b>
2.1: Energy ratios depending on the ram and drop mechanism.	10
2.2: Overburden pressure correction factors.	10
2.3: Drill diameter, tube type, rod length and impact rate correction factors.	11
3.1: Soil classes.	28
5.1: Correlations Based on $q_c$ -N Relationship.	34
5.2: Suggested $(q_c/Pa)/N_{60}$ ratios.	37
5.3: Correlations Based on Mean Grain Size, $D_{50}$ .	38
5.4: Correlations Based on Fines Content, FC%.	39
5.5: Correlations Based on Soil Behavior Type Index, $I_c$ .	39
6.1: The equations selected to be used in this study.	48
6.2: The equations proposed in this study.	57

# 1. INTRODUCTION

The Northern Marmara Highway, KMO, is an uninterrupted transportation corridor that was constructed to alleviate the heavy traffic of the Marmara Region, which hosts the largest industrial zones of Turkey. The KMO, which connects Asia and Europe, is also called as Highway 7. Highway 7 is a four-lane highway in each direction therefore, it has tunnels with the 4-lane which are widest highway tunnels in the world.

The KMO, which is a total of 400 km long, starts from Kınalı junction in Silivri district on the European side of Istanbul. It ends in Odayeri district of Eyüp district (Figure 1.1), which is connected to Yavuz Sultan Selim Bridge (Figure 1.2) for the Bosphorus crossing (Figure 1.2), including the connection roads of Istanbul Airport. The Habibler-Hasdal junction, another branch of the KMO on the European side, provides an alternative to city traffic. The route of the KMO on the Asian side of Istanbul starts from Kurtköy and continues uninterruptedly until Akyazı. Along this route, Sabiha Gökçen Airport, Istanbul Park, Gebze OSGB, Dilovası TEM connection road, D-100 connection road, Osmangazi Bridge and Izmit are easily accessible (Figure 1.1).

The main engineering structures of the Northern Marmara Motorway are viaducts, tunnels, overpasses, underpasses and culverts. A total of 14 viaducts, 37 bridges, 3 tunnels, 19 overpasses, 43 underpasses and 118 culverts were constructed in the European parts of the project. In the Asian parts, a total of 16 viaducts, 106 bridges, 5 tunnels, 54 overpasses, 53 underpasses and 481 culverts were constructed.

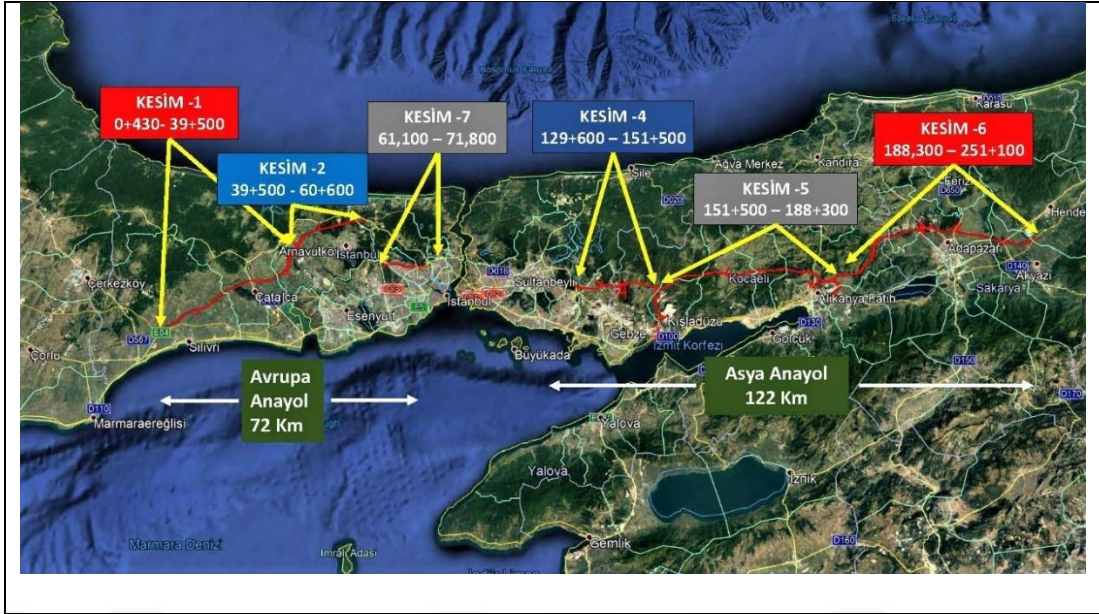


Figure 1.1: Northern Marmara Motorway Route.



Figure 1.2: Yavuz Sultan Selim Bridge.

The KMO is a comprehensive transportation project built in a total of 7 separate sections (Figure 1.1). The Section 6 of the KMO project, which is the eastern most segment (Figure 1.1) consists of approximately 8 km of tunnels and more than 3 km

of viaducts (Figure 1.3). In addition, a total of 73 bridges (Figure 1.4), 11 intersections (Figure 1.5), 35 overpasses (Figure 1.6), 19 underpasses and 162 culverts (Figure 1.7) were constructed in this section. Photos from Figures 1.4 through 1.7 were provided by the KMO management office.



Figure 1.3: A viaduct at the region 6 of the KMO.



Figure 1.4: A bridge at the region 6 of the KMO.



Figure 1.5: A partial cloverleaf interchange at the region 6 of the KMO.



Figure 1.6: An overpass at the region 6 of the KMO.



Figure 1.7: A partial cloverleaf interchange with an underpass and hydraulic culvert at the region 6 of the KMO.

The predominant subsurface soil profile of the Section 6 composes of compressible soft soil sites including silty clays, clayey silts and clays which are classified as transitional soils [Schneider et al., 2008]. Therefore, the design team of the KMO implemented various geotechnologies to mitigate the settlement and bearing capacity concerns for the construction of the engineering structures and embankments. They have performed a comprehensive subsurface investigation program including Standard Penetration Test (SPT) borings, pressuremeter tests (PMT), Cone Penetration Tests with pore water pressure measurements, piezocone tests (CPTu), and laboratory tests.

The Standard Penetration Test was developed by Raymon Pile Company in the 1920s [Bowles, 1988], standardized by the ASTM [ASTM D1586] and is widely used all over the world to estimate soil properties. The number of blows is counted to penetrate a standard SPT split-spoon sampler 30 cm into the soil using a hammer weighing 63.5 kg which is dropped from a height of 76 cm. The standard CPTu test measures tip stress,  $q_c$ , sleeve friction,  $f_s$ , and dynamic pore water pressure,  $u_2$ , while the CPTu probe advances into the subsurface continuously.

While the CPTu providing continuous data through the subsurface profile, SPT is traditionally performed on 1 m to 1.5 m intervals. The CPTu is operator independent, therefore, the repeatability is more reliable comparing to that of SPT. On the other hand, disturbed soil samples can be collected by SPT. Therefore, both SPT and CPTu are used together for geotechnical site investigation projects to construct the idealized soil profile of the site. Consequently, there is a wealth of published correlation in the literature on estimating SPT blow counts using CPTu data. One of the objectives of the thesis is to analyse the predictive performances of the existing equations on transitional soils encountered in the Section 6 of the KMO.

Both SPT and CPTu testing techniques were explained in the Chapter 2, the prediction of the soil behavior type (SBT) based on CPTu data is discussed in the Chapter 3 and the geology of the Region 6 alignment was evaluated in the Chapter 4. SPT and CPTu testing program was explained in the Chapter 5 in detail. In addition, equations for predicting the SPT blow counts of transitional soil were proposed in the Chapter 6.

## **2. SPT-CPT CORRELATION**

### **2.1. Standard Penetration Tests (SPT)**

The standard penetration test (SPT) is one of the oldest field experiments since the year it was introduced. There are various advantages of the SPT when compared to other in-situ soil characterization techniques. It is simple to conduct, has a low cost compared to other experiments. It is applicable on most of the soils and underground water level. It provides the opportunity to take disturbed samples from the soil [Nixon, 1982]. Thanks to the advantage of disturbed sampling, physical soil properties such as Atterberg limits, grain size distribution, moisture content and specific gravity can be determined. SPT is also frequently performed in Turkey because there are many higher frequencies of over consolidated clays and sandy soil profiles in the geotechnical investigations [Durgunoğlu and Toğrol, 1974]. The SPT data are used in various geotechnical design calculations such as liquefaction potential, bearing capacity and settlement predictions.

In 1958, the test procedure method was standardized by the ASTM [ASTM D1586], and it has reached today with a few changes.

#### **2.1.1. Experimental Procedure**

A ram weighing 63.5 kg is dropped from a height of 76 cm in the SPT. This procedure is shown in Figure 2.1 [Coduto, 1994]. The SPT split-spoon sampler is attached to the end of the rods and lowered to the bottom of the drilling and hammered into the ground 45 cm.

The number of blows of the first 15 cm is not taken into account due to the disturbance of the drilling base and the sum of the blow numbers of the last two 15 cm penetrations is recorded (SPT-N or N). This is shown in Figure 2.2 [FHWA, 2002]. If the number of blows required for 30 cm penetration exceeds 50 or no progress is made in the first 10 blows, the test is stopped, the number of blows and the penetration amount are recorded [Ulusay, 2010].

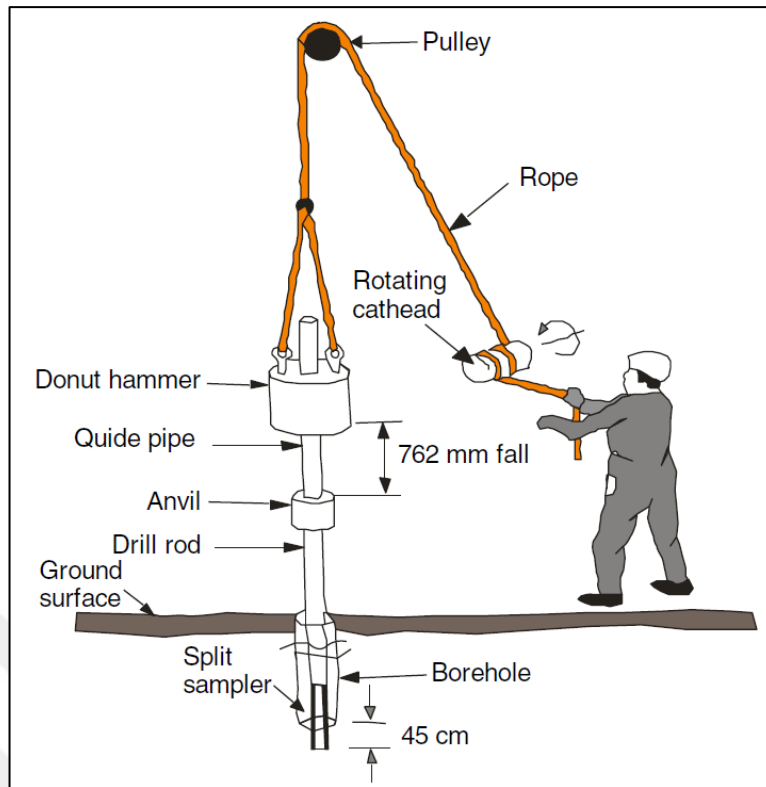


Figure 2.1: Performing the standard penetration test.

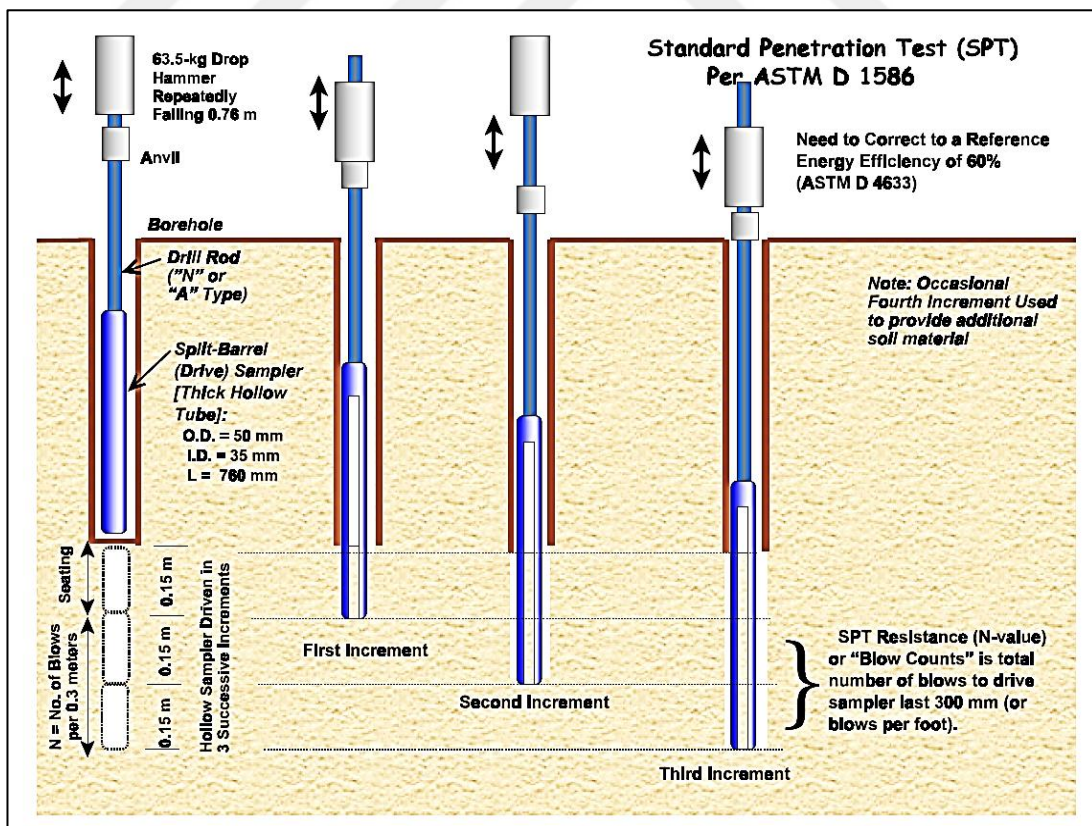


Figure 2.2: Standard penetration test steps.

## 2.1.2. Factors Affecting SPT Results and Corrections

How the SPT test is conducted, and equipment is of great importance to achieve correct results. Therefore, the hammer type and release method used in the SPT cause the ratio of the energy transmitted to the end of the split spoon sampler to the input energy ( $E_R$ ) to change. The relationship between hammer type, release method and energy ratio differ between countries [Clayton et al., 1995] (Table 2.1). Although the same field conditions are provided, different numbers of blow counts are observed due to other factors. This situation causes the reliability and usability of the experiment to be questioned [Coduto, 1994]. In addition, factors such as the diameter of the borehole, whether the liner is used together with the standard split spoon sampler, the rod length, and the effective stress directly affect the test results. Due to these mentioned effects, the SPT-N value recorded in the experiment is expected to be corrected according to the energy ratio and other listed factors above. The 60% energy ratio, which is considered the standard to get a more accurate value, has been proposed by Seed et al., (1984). The corrected SPT-N value is named  $N_{60}$  and  $(N_1)_{60}$  and is shown below. The influence factors are provided in Tables 2 [Liao and Whitman, 1986] and 3 [Aggour and Radding, 2001].

To calculate the  $N_{60}$ , in addition to Equation 2.1, the use of the factors of blow count frequency, hammer head and hammer pad was suggested by McGregor and Duncan (1998). These factors are included in Equation 2.2.

$$N_{60} = \frac{E_R C_B C_S C_R N}{60} \quad (2.1)$$

$$N_{60} = \frac{E_R C_B C_S C_R C_A C_C C_{BF} N}{60} \quad (2.2)$$

$$(N_1)_{60} = C_N N_{60} \quad (2.3)$$

where;

$N_{60}$  is corrected SPT N-value,  $E_R$  is hammer efficiency,  $C_B$  is borehole diameter correction,  $C_S$  is sampling method correction,  $C_R$  is rod length correction,  $C_N$  is

overburden stress correction factor,  $C_A$  is casing head correction,  $C_C$  is hammer pad correction and  $C_{BF}$  is hammer blow count frequency correction.

Table 2.1: Energy ratios depending on the ram and drop mechanism.

Country	Hammer type	Release mechanism	Average rod energy ratio (%)
Argentina	Donut	Cathead	45
Brazil	Pin weight	Hand dropped	72
China	Automatic donut	Hand trip	60
	Donut	Dropped	55
	Donut	Cathead	50
Colombia	Donut	Cathead	50
Japan	Donut	Tombi	78-85
	Donut	Cathead, 2 turns + special release	65-67
UK	Automatic	Trip	73
USA	Safety	Cathead, 2 turns	55-60
	Donut	Cathead, 2 turns	45
Venezuela	Donut	Cathead	43

Table 2.2: Overburden pressure correction factors.

Researchers	Correction factor $C_N$	Units of $\sigma_v^t$
Teng (1962)	$C_N = \frac{50}{10 + \sigma_v^t}$	psi
Peck,Hansen and Thornburn (1974)	$C_N = 0.77 \log\left(\frac{20}{\sigma_v^t}\right)$	ton/ft <sup>2</sup>
Seed (1976)	$C_N = 1 - 1.25 \log(\sigma_v^t)$	ton/ft <sup>2</sup>
Tokimatsu and Yoshimi (1983)	$C_N = \frac{1.7}{0.7 + \sigma_v^t}$	kgf/cm <sup>2</sup>
Liao and Whitman (1986)	$C_N = \left(\frac{1}{\sigma_v^t}\right)^{0.5}$	kgf/cm <sup>2</sup>

Table 2.3: Drill diameter, tube type, rod length and impact rate correction factors

Variables		Correction Factors				
		Symbols	Skempton (1986)	Robertson and Wride (1997)	McGregor and Duncan (1998)	Bowles (1996)
Rod Length	> 30 m	$C_R$	1	< 1.0	1	1
	10 – 30 m		1	1	1	1
	6 – 10 m		0.95	0.95	1	0.95
	4 – 6 m		0.85	0.85	1	0.85
	3 – 4 m		0.75	0.75	1	0.75
	0 – 3 m		0.75	-	0.75	0.75
Tube	If a non-lining sample receiver is used	$C_S$	1.2	1.1-1.3	-	1.0
	Standard tube (with liner) sample receiver:		1	1	-	0.9
	Loose sand Dense sand and clay		1	1	-	0.8
Borehole diameter	60 – 120 mm	$C_B$	1	1	-	1
	150 mm		1.05	1.05	-	1.05
	200 mm		1.15	1.15	-	1.15
Hammer blow count frequency	Less than 20 and 10-20 blow / min	$C_{BF}$	-	-	0.95	-
	More than 20 and 10-20 blow / min		-	-	1.05	-

## 2.2. Piezocone Tests (CPTu)

The cone penetration test (CPT) was first used in the Netherlands in 1934 to determine the properties of sand layers for pile design [Erol and Çekinmez, 2014]. Later, it spread all over the world and reached a widespread utilization. CPT stands out because it provides continuous data and is fast and practical in determining the soil properties and profiles, works by measuring the resistance at probe tip (tip stress)  $q_c$ ,

and probe sleeve (sleeve resistance),  $f_s$ , as a result of pushing a conical tip to the soil at a constant speed. Later in 1974, pore pressure sensor was introduced to capture pore pressures (piezocone, CPTu) while the cone penetration [Robertson and Cabal, 2015]. The location of the pore pressure sensor behind the cone tip is now an industry standard and pore water pressures recorded behind the tip is called as  $u_2$ .

Starting from the 1970s, the CPT used in alluvial ground in Turkey [Durgunoğlu and Toğrol, 1974]. There are several international standards for this experiment, one of which has been developed by the American Society for Testing and Materials [ASTM D3441].

CPTu can be performed in a wide range soil from clayey to sandy soils, but it is not suitable for use on gravel and rock soils [Durgunoğlu and Toğrol, 1974]. Thanks to the detailed continuous data recording, the role of the CPTu in subsurface investigations has been listed by Erol and Çekinmez (2014) as follows:

- Determination of the soil profile
- Determination of groundwater level
- Pore water pressure estimation
- Estimation of physical and mechanical properties of soil layers
- Settlement and bearing capacity approaches on shallow and deep foundations.
- Liquefaction potential assessments
- Quality control in soil improvement applications
- Seismic wave velocity measurements

CPT probe is shown in Figure 2.3 [Robertson and Cabal, 2014].



Figure 2.3: CPT probes.

### 2.2.1. Types of CPT

CPT systems are examined in four main groups: mechanical, electrical, piezocone (CPTu) and seismic cone penetrometers (SCPTu).

### 2.2.2. Mechanical Cone Penetrometers

The mechanical cone penetrometer experiment, which was first used in the Netherlands in the 1930s, is done by manually pushing a mechanical cone with a projection area of  $10 \text{ cm}^2$  and a  $60^\circ$  apex angle. This is shown in Figure 2.4 [Robertson and Cabal, 2014]. The cone is mounted on the end of a 15 mm diameter steel pipe that passes through a 35 mm outer diameter pipe [Sanglerat, 1972, Lunne, et al., 1997]. A lateral shaft was added to this cone by Begemann (1953) to measure the friction resistance. This is shown in Figure 2.5 [Robertson and Cabal, 2014].

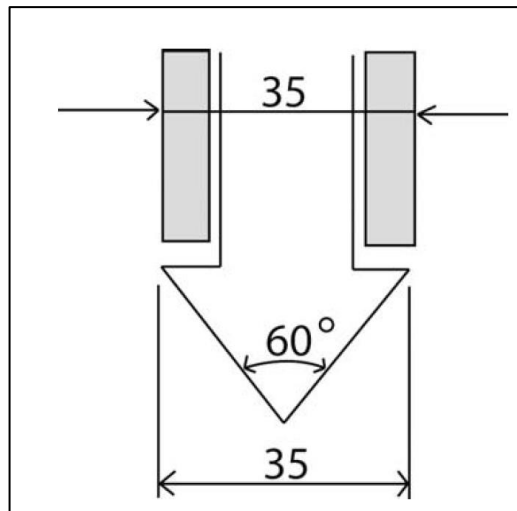


Figure 2.4: Mechanical cone.

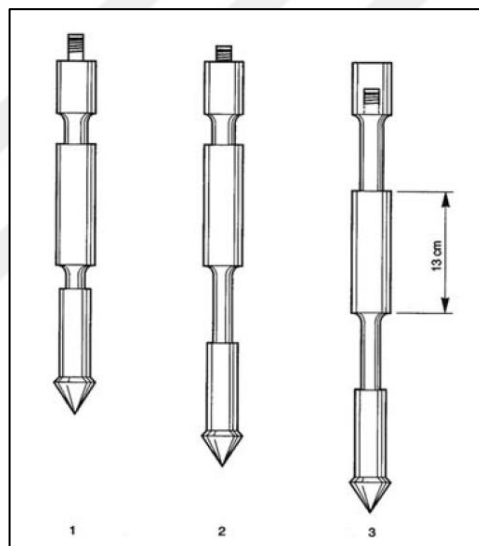


Figure 2.5: Begemann type cone with friction sleeve.

### 2.2.3. Electric Cone Penetrometers

It was produced in the Delf soil mechanics laboratory in the 1950s [Vlasblom, 1985]. With the help of sensors located on the cone part of the electronic CPT penetrometer, the tip resistance and friction resistance are measured without incision. [Lunne et al., 1997] (Figure 2.6).

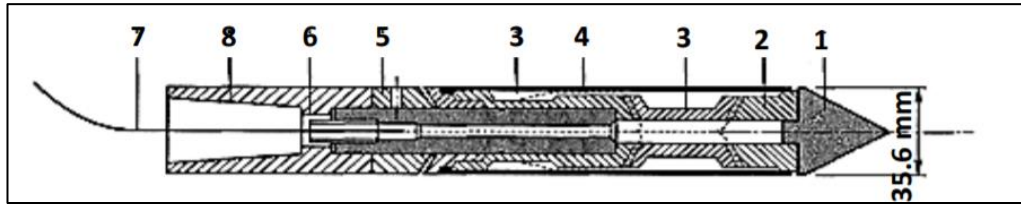


Figure 2.6: Piezometric Electric CPT (CPTu)

Piezometric CPT, piezocone, CPTu, which can measure pore water pressure, emerged in 1974 at the Norwegian Geotechnical Institute. In 1975, Torstensson in Sweden and Wissa et al., (1975) in the USA developed an instrument that can measure resistances and pore water pressure together [Lunne et al., 1997]. It is a common method that enables to find soil properties and profiles in a fast and uninterrupted manner [Özer et al., 2010]. The pore water pressures measured in this test are dynamic pressures, but the test can be stopped at the desired depth and static pore water pressures can be measured. Electric piezometric cone penetrometer is shown in Figure 2.7 [Web 2, 2022].



Figure 2.7: Electric piezometric cone penetrometer.

## 2.2.4. Seismic CPT (SCPTu)

In Seismic Piezometric Electric CPT (SCPTu), geophones are placed on the test probe and seismic waves are created by hammer blows from the ground surface. These created waves are detected by the receiver in the probe, and seismic wave velocities are measured with these data on the computer, and interpretations can be made about soil properties by means of obtained wave velocities. In addition, many wave velocity measurements are possible by stopping penetration at desired depths during the experiment. Seismic CPT (SCPTu) is shown in Figure 2.8 [Web 3, 2022].

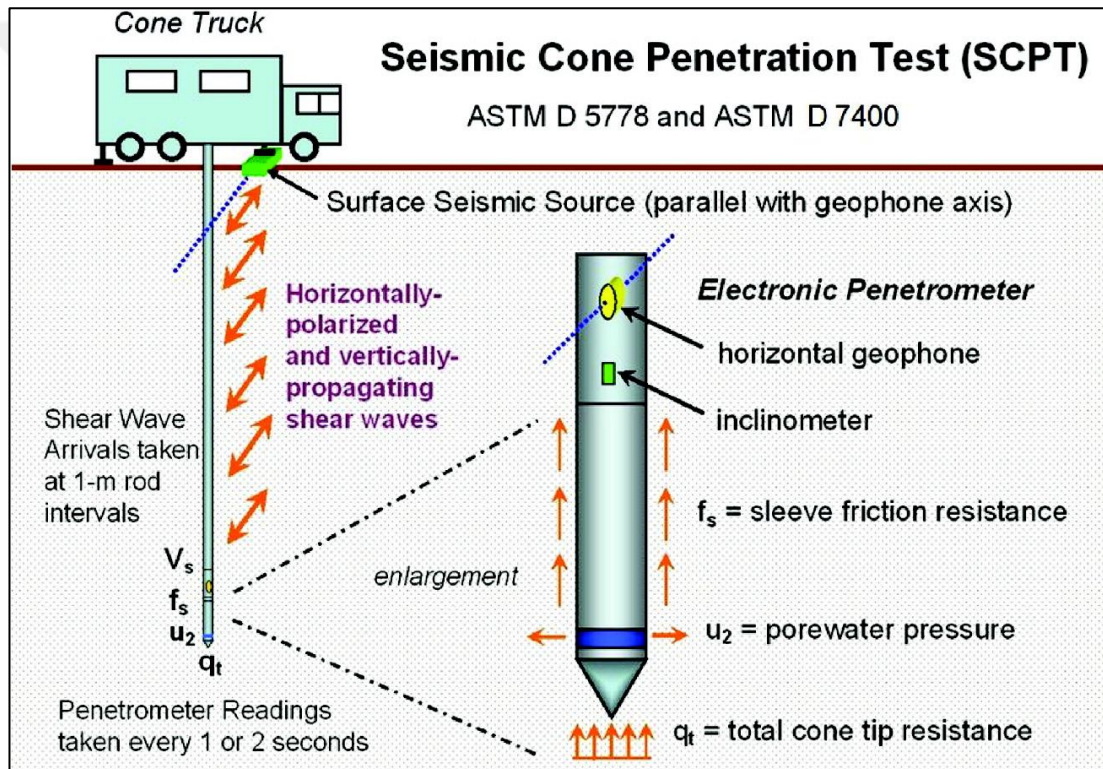


Figure 2.8: Seismic CPT (SCPTu).

## 2.2.5. Data Obtained by CPTu

Tip resistance ( $q_c$ ), sleeve friction resistance ( $f_s$ ), dynamic and static pore water pressures ( $u$ ) are recorded using CPTu. The definitions of the parameters and evaluations of their physical meanings are given below.

Tip resistance ( $q_c$ ): It is defined as the ratio of soil reaction force measured at the tip of the cone penetrometer to the cross-sectional area in the experiment.

Sleeve friction resistance ( $f_s$ ): It is the ratio of the force measured at the friction shaft surface to the friction rod surface area.

Pore pressure ( $u_2$ ): The pore pressure generated during cone penetration when measured behind the cone.

Corrected tip resistance ( $q_t$ ): It is the corrected tip resistance for the effect of pore water pressure.

$$q_t = q_c + u_2(1 - a) \quad (2.4)$$

Where  $a$  is the cone area ratio, it is between 0.50 and 1.00

Normalized cone resistance ( $Q_t$ ): This is the normalised cone resistance taking overburden load into account.

$$Q_t = \frac{q_t - \sigma_{v0}}{\sigma'_{v0}} \quad (2.5)$$

where,  $\sigma_{v0}$  and  $\sigma'_{v0}$  are total and effective overburden stresses, respectively.

Friction ratio ( $R_f$ ): It is the ratio of the friction resistance measured at the same depth to the cone tip resistance.

$$R_f(\%) = \left( \frac{f_s}{q_c} \right) \times 100 \quad (2.6)$$

Normalized Friction Ratio ( $F_r$ ):

$$F_r(\%) = \left( \frac{f_s}{q_c - \sigma_{v0}} \right) \times 100 \quad (2.7)$$

Excess pore pressure, net pore pressure ( $\Delta u$ ): The measured pore pressure minus the in-situ equilibrium pore pressure.

$$\Delta u = u_2 - u_0 \quad (2.8)$$

Pore pressure ratio ( $B_q$ ): The net pore pressure normalized with respect to the net cone resistance.

$$B_q = \frac{\Delta u}{q_n} \quad (2.9)$$

Net cone resistance ( $q_n$ ): The corrected cone resistance minus the vertical total stress.

$$q_n = q_t - \sigma_{v0} \quad (3.1)$$



### **3. SOIL BEHAVIOUR TYPE**

One of the interpretations of CPTu is soil profiling and soil type. CPTu tip resistance is high in sands and low in clays. In addition, friction ratio is low in sands and high in clays. CPTu is not expected to provide physical properties of soil types. However, CPTu is expected to provide conditions such as soil behaviour type (SBT) using mechanical characteristics of soils measured by CPTu. CPTu data allows to obtain the repeated mechanical behaviour of the soil around the probe [Robertson and Cabal, 2014].

#### **3.1. Non-Normalized SBT Charts**

A SBT chart was proposed by Robertson et al. (1986). A dimensionless version of this chart was updated by Robertson (2010). This chart is shown in Figure 3.1 [Robertson, 2010]. In this chart, tip resistance and friction ratio are used. It is recommended that, this chart can provide SBT estimation to a depth of approximately 20 meters. Local experiences and overlaps may be altered in some areas [Robertson and Cabal, 2014].

#### **3.2. Normalized SBT (SBT<sub>n</sub>) Charts**

When effective overburden stress increases, penetration resistance and sleeve resistance also increase with depth. Therefore, it is necessary to normalize the CPTu data for overburden stress. In this context, the most commonly used soil behaviour chart based on normalized CPTu data was proposed by Robertson (1990). This chart shown in Figure 3.2 [Robertson, 2010] which indicates an area where most young, uncemented, insensitive, normally consolidated soils. Also, ground response, overconsolidation ratio, age, and cementation for sandy soils, increasing stress history, and soil sensitivity for cohesive soils are considered.

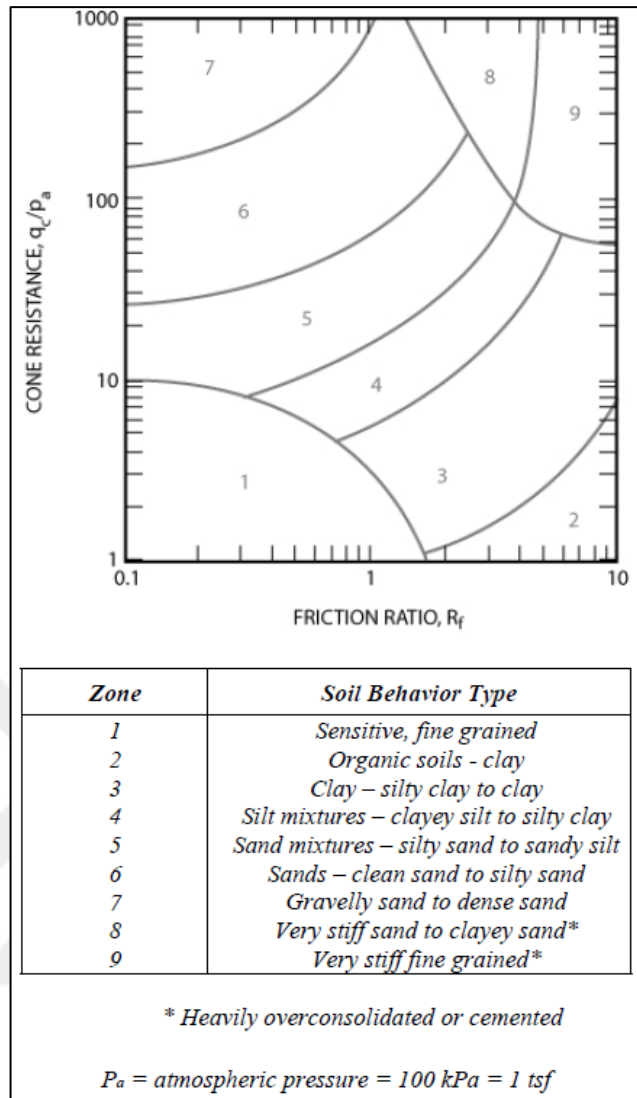


Figure 3.1: Non-normalized CPT Soil Behavior Type (SBT) chart.

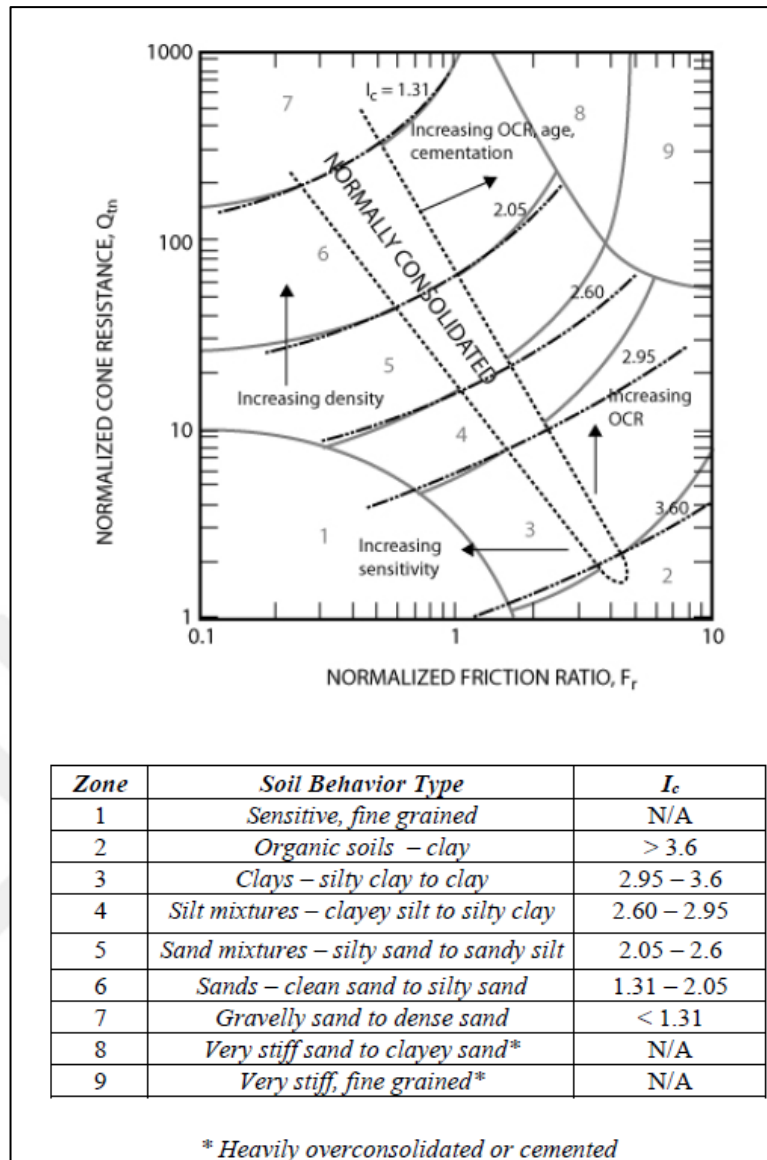


Figure 3.2: Normalized CPT Soil Behavior Type (SBT) chart.

Robertson 1990 also provided the SBTn charts as a function of the normalized pore pressure parameter ( $B_q$ ). These charts are shown in Figure 3.3.

The  $Q_t$ - $B_q$  chart can be used to determine soft, saturated fine-grained soils where the  $CPT_u$  pore pressure is high. Typically, this chart is not used in onshore areas because repeatable pore pressure results are scarce [Robertson and Cabal 2014].

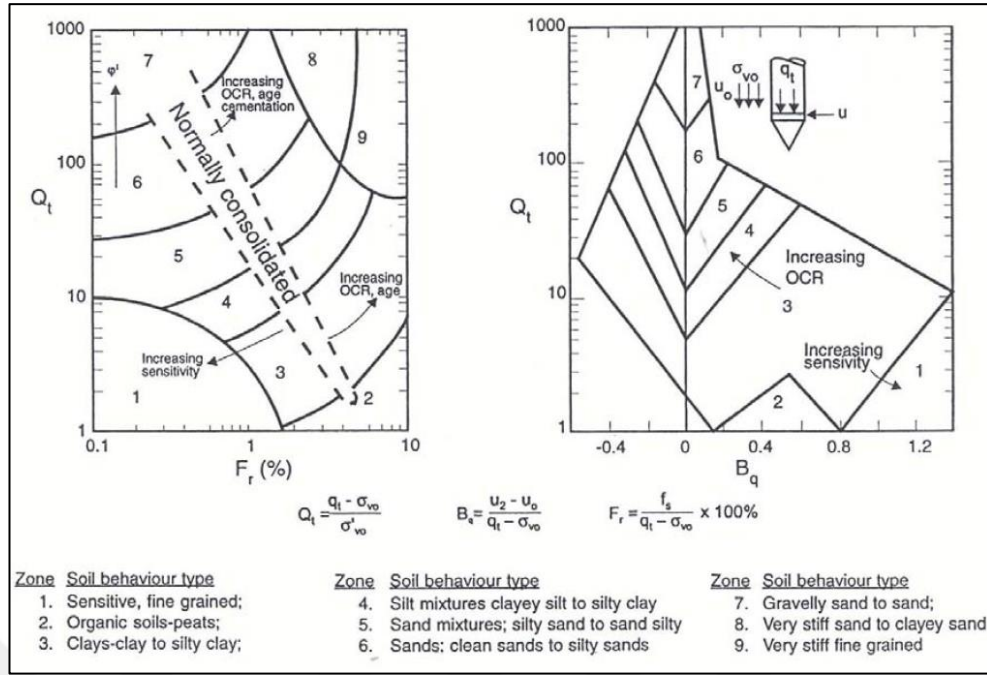


Figure 3.3: Normalized CPT Soil Behavior Type (SBT<sub>n</sub>) charts  $Q_t - F_r$  and  $Q_t - B_q$

Physical soil samples are required to perform soil classification test to classify soil types. However, if a CPTu experiment has been conducted the soil behaviour types can be determined [Robertson and Cabal, 2014].

When the pore pressure data measured, the soil behaviour type can be determined (Figure 3.3). The penetration pore pressures may be high for soft clays on the other hand in stiff, heavily over-consolidated clays or silts and silty sands, the penetration pore pressures ( $u_2$ ) may be low and occasionally negative relative to the static pore pressures ( $u_0$ ) [Robertson and Cabal, 2014]. Excess pore pressure dissipates quickly in sandy soils, while it occurs slowly in clayey soils. Therefore, the soil type can be determined by the dissipation rate of the pore pressure when the test is stopped.

According to the SBT chart that Robertson mentioned in 1990 and then updated by Robertson (2010) (Figure 3.2), normalized cone penetration resistance and normalized friction ratio were combined into the Soil Behaviour Type Index,  $I_c$ , [Robertson and Cabal, 2014]. Accordingly, the following equation is defined:

$$I_c = ((3.47 - \log Q_t)^2 + (\log F_r + 1.22)^2)^{0.5} \quad (3.4)$$

Where,  $Q_t$  is normalized cone penetration resistance (dimensionless), and  $F_r$  is normalized friction ratio (%)

The  $I_c$  boundaries shown in Figure 3.2 provide information about the soil types. The soil behaviour type index does not apply to zones 1, 8 and 9 in the chart. In addition, studies have shown that the chart in Figure 3.2 gives 80% more reliable results [Robertson and Cabal, 2014].

### **3.3. Transitional Soil**

Schneider et al., (2008) published an article on soil classification based on CPTu results. They show that the well-known and widely used Robertson (1990, 1991) charts for postprocessing results may not be able to correctly classify when there are additional complexities in soil behaviour. Clays, silty clays were represented by Robertson as zone 3, they suggested that a heavily over consolidated clay would not behave the same as a normally consolidated silty soils and therefore should not have the same "soil behaviour type" based on the piezocone response. As an example of this, North Sea clay data Ramsey (2002) compared in the Robertson's chart and showed that these clay soils are distributed in 5 different regions [Schneider et al., 2008] (Figure 3.4).

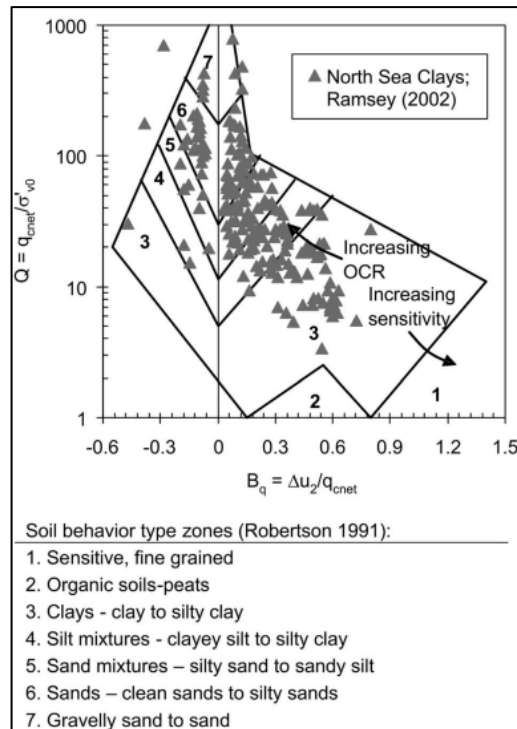


Figure 3.4: Location of North Sea clay data of Ramsey (2002) superimposed on Robertson's (1990) chart.

Schneider et al. (2008) mentioned about these effects that may cause misclassification when performing soil classification using normalized cone tip resistance and normalized excess pore pressures. It has been stated that effects such as the rate of penetration, whether the penetration is drained, undrained or partially drained, and the rate of consolidation should be taken into account for soil behaviour classification.

For this reason, Schneider et al., (2008) created charts using field data of drained sand, sensitive clay, silt or silty soils. Schneider et al., (2008) was noted that some of the drained sands with a low  $Q$  value approach the boundaries of silty sand with drainage. It defined soils such as clayey sands and silts, silty clays and many residual soils as transitional soils as shown in Figure 3.5 [Schneider et al., 2008].

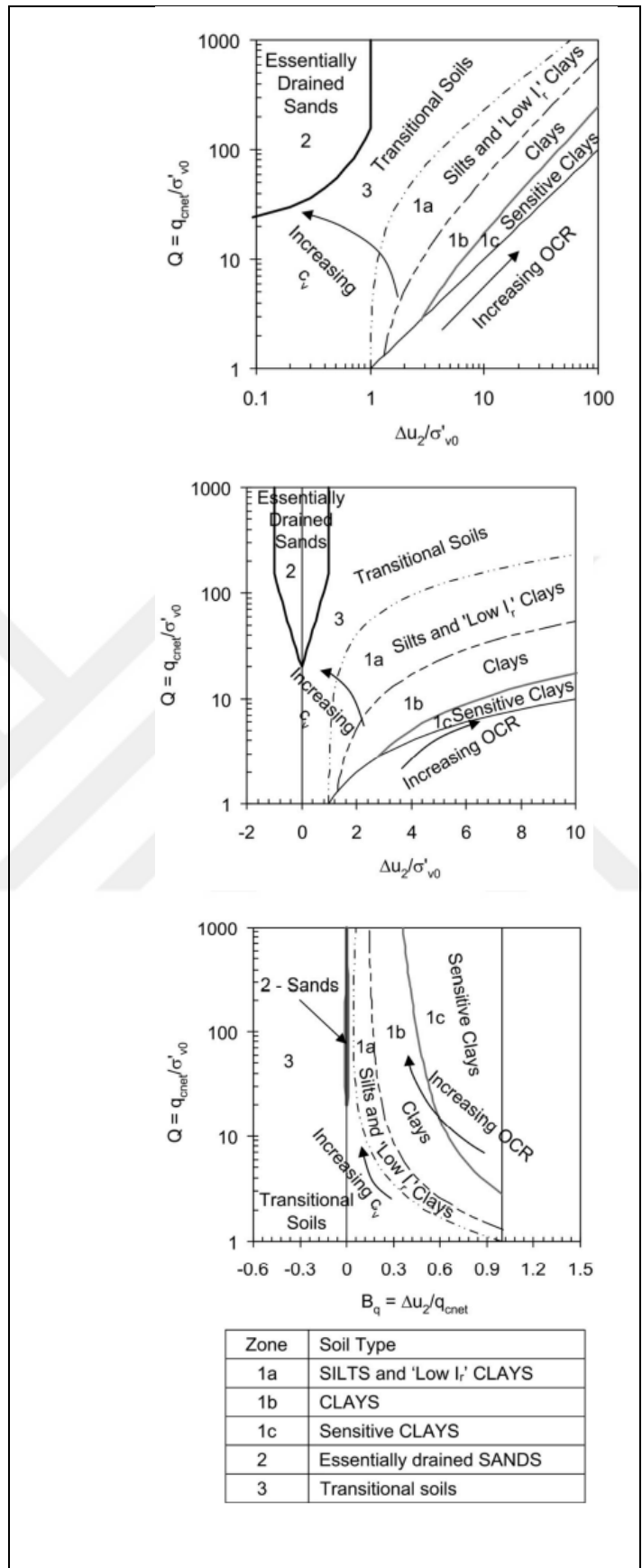


Figure 3.5: Soil classification charts.

It is noted that the “regions” in these three graphs are the same, but the graphs are shown in different formats: log–log  $Q-\frac{\Delta u_2}{\sigma'_{vo}}$ , semi log  $Q-\frac{\Delta u_2}{\sigma'_{vo}}$ ; and semi log  $Q-B_q$ . Based on Schneider et al. (2008):

Zone 1: Clays, clayey silts, silts, sandy silts and sands with positive excess pore pressures,

Zone 2: Sand and transitional soils with low negative excess pore pressures,

Zone 3: Clayey soils with high negative excess pore pressure.

Schneider et al. (2008) compared their classification with the Robertson (1990) chart in Figure 3.6 [Schneider et al., 2008].

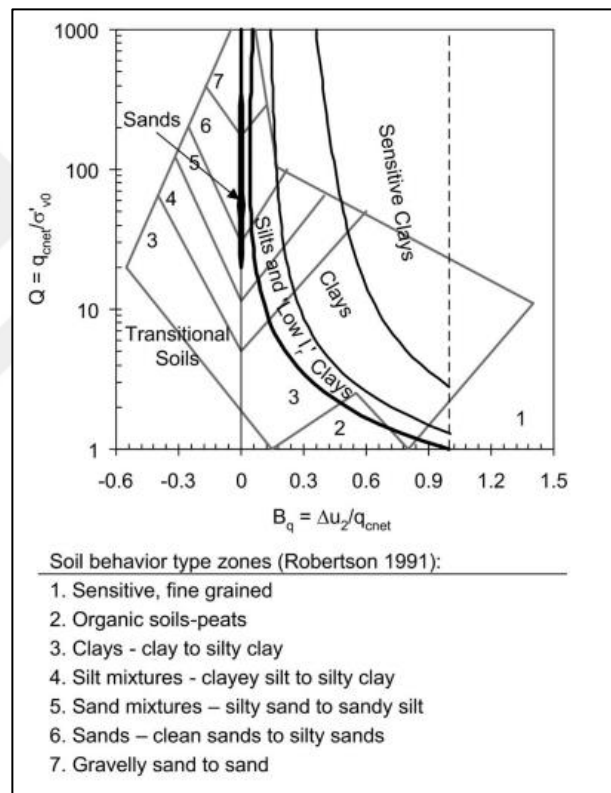


Figure 3.6: Comparison of chart proposed by Schneider et al., 2008 with Robertson (1990).

Schneider et al., (2008) pointed out that correlations created using drained or completely non-drained soils will have lower reliability for transitional soils (Figure 3.6).

A recent soil classification study was conducted by Bol (2013) using the comprehensive database performed in Adapazarı soils. Bol (2013) proposed the  $I_c$  equation as a function of dynamic porewater pressure gradient,  $i$  (Equation 3.5), using

CPTu experimental data. The  $i$  increases with the liquid limit increases and decreases with the grain size increase. In addition, the clayey soils exhibit positive  $i$  values whereas silts, dense sands and clays with low plasticity exhibit negative  $i$  values (Figure 3.7) [Bol, 2013]. A soil classification chart composes of a total of 7 regions (Figure 3.7 and Table 3.1) is proposed based on  $I_c$  (Equation 4.2) [Bol, 2013].

$$i = \frac{\Delta u_2}{\Delta \sigma_0} = \frac{u_{2z_2} - u_{2z_1}}{(\sigma_{0z_2} - \sigma_{0z_1})} \quad (3.5)$$

$u_{2z_2}$  and  $u_{2z_1}$  are the porewater pressures corresponding to depths  $z_2$  and  $z_1$  and  $\sigma_{0z_2}$  and  $\sigma_{0z_1}$  are total stresses at depths  $z_2$  and  $z_1$  respectively.

$$I_c = \sqrt{\{3.47 - 0.9 \log[Q(1 - 0.01i)]\}^2 + \{1.4 + 2[\log F / (1 - 0.01i)]\}^2} \quad (3.6)$$

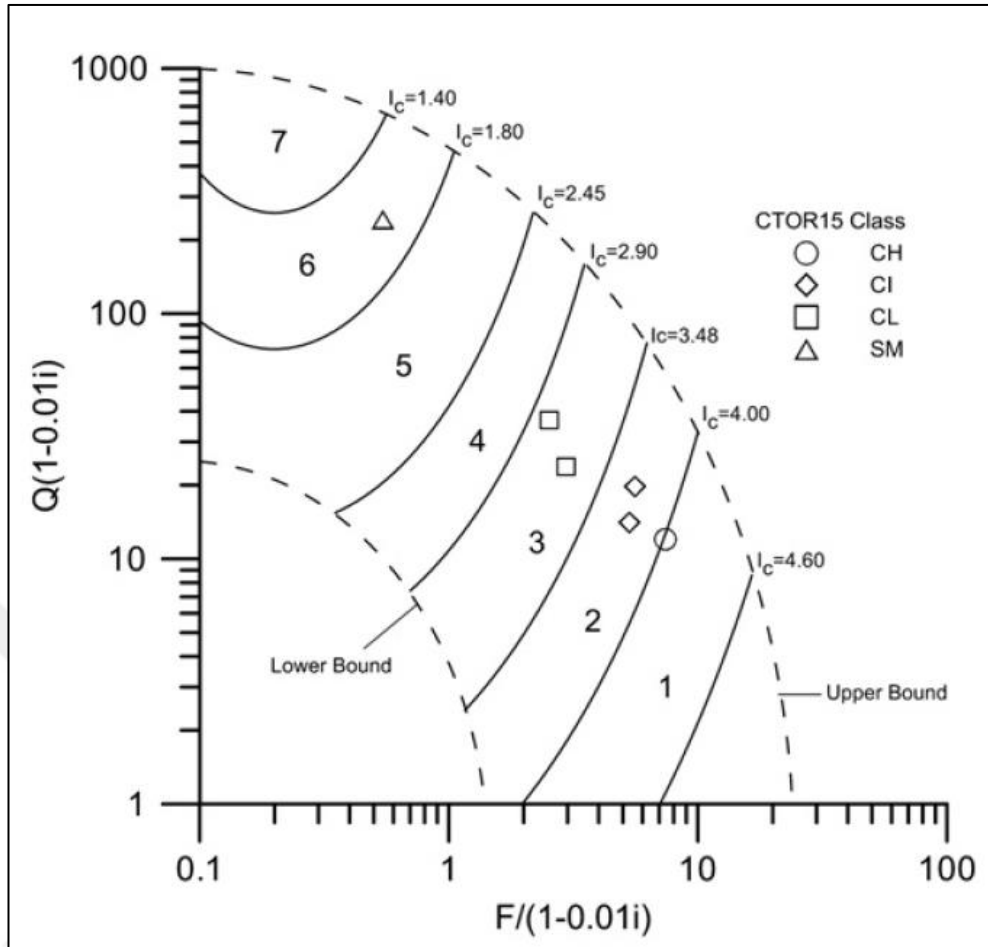


Figure 3.7: Soil classification chart.

Table 3.1: Soil classes.

Zone	$I_c$	Soil class
1	$I_c < 1.4$	SP or gravels
2	$1.40 < I_c < 1.8$	SW-SM or SP-SM
3	$1.80 < I_c < 2.45$	SM or ML
4	$2.45 < I_c < 2.90$	CL or ML
5	$2.90 < I_c < 3.48$	CI-MI or CL
6	$3.48 < I_c < 4$	CH or CI
7	$I_c > 4.00$	CH

## 4. GEOLOGY of THE STUDY AREA

The Section 6 of the KMO project, which is the eastern most segment starts from east of Kocaeli and ends in Akyazı/Sakarya (Figure 1.1). Kocaeli-Adapazarı consists of four different areas (the Kocaeli Peneplain in the north, the İzmit–Sapanca Trough, the Adapazarı Depression in the middle, and the Samanlı–Kapıorman Mountains in the south) in terms of morphology. These four regions are shown in Figure 4.1 [Tari and Tüysüz, 2016].

The first of these four regions is the Kocaeli Peneplain, located in the north. Kocaeli Peneplain has approximate height of 150-200 meters. Despite it is not known exactly when this peneplain existed, it is suggested that it occurred in the Late Miocene age by comparing it with similar formations found in Anatolia. At the same time, it forms an asymmetrical and inclined structure towards the Black Sea [Tari and Tüysüz, 2016].

The second region is the İzmit–Sapanca Trough. This trough is a young trough filled with alluvial material derived from the Samanlı Mountains in the south. It contains Sapanca Lake in the depression which is the continuation of İzmit Bay [Tari and Tüysüz, 2016].

The third region is Adapazarı Depression is located between 3 regions. There is İzmit-Sapanca Trough in the west, Kocaeli Peneplain in the north, Kapıorman Mountains in the south. It is filled with alluvials carried by the rivers. The southern boundary of this region was determined as the northern branch of the North Anatolian Fault line, ruptured on 17 August 1999.

The fourth region is formed by the Samanlı Mountains and its eastern side by the Kapıorman Mountains. The heights of these mountains can reach up to 900 m and 1600 m, respectively [Tari and Tüysüz, 2016].

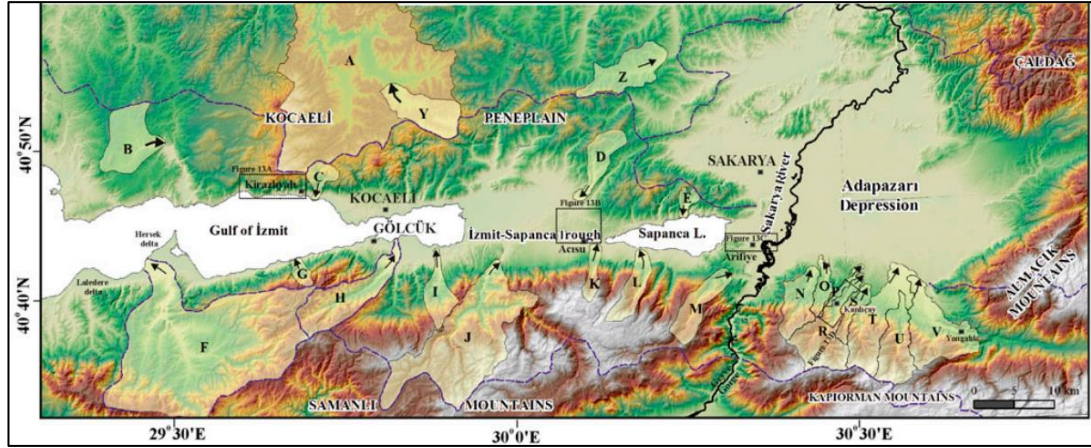


Figure 4.1: Morphology of the region.

In Kocaeli - Adapazarı Region, where the North Anatolian Fault Line extends along the south of the Marmara Sea. This is shown in Figure 4.2 [Tari and Tüysüz, 2016]. The soil profile contains very thick, soft to medium solid clay or loose sand layers. The area between Adapazarı Plain and Sapanca Lake - İzmit Bay is covered with alluvial material, which makes the soil conditions unfavorable.

Bol (2003) mentioned that Adapazarı city is a typical plain city on an alluvial fill (Figure 4.2) [Bol, 2003]. Adapazarı plain was formed under the influence of some external forces (Figure 4.3, [Web, 4]) (Sakarya River, which takes its source from the Geyve Strait, Çark Stream connected to Sapanca Lake, and Mudurnu Stream reaching the Adapazarı plain from the Mudurnu valley). With the alluvial material carried by these rivers, Adapazarı Plain forms a nearly horizontal and thick alluvial layer. The thickness of this alluvial layer reaches up to 1000 meters [Komazawa, et al., 2002].

Adapazarı basin, approximately 1000 years old, is about close to the city center and has a depth of 400 meters [Bray et al., 2004].

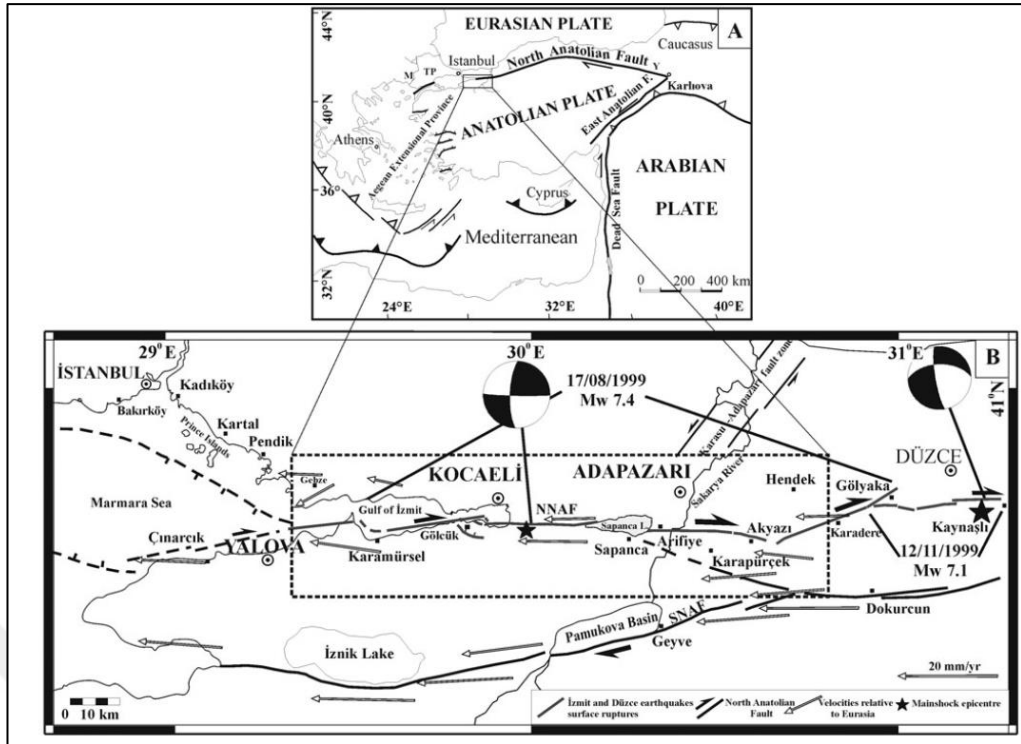


Figure 4.2: North Anatolian Fault Line.

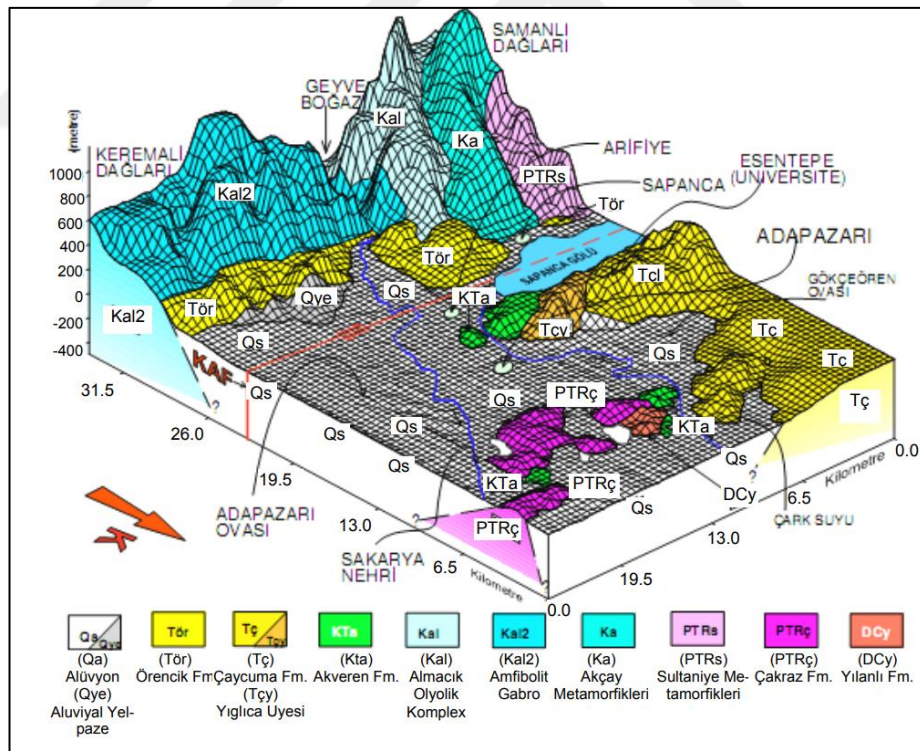


Figure 4.3: Geomorphology and geology of Adapazarı.



Figure 4.4: Sakarya River.

Various studies have been carried out on the Adapazari region. Sancio et al., (2002) conducted a total of 46 SPT and 135 CPTu experiments. As a result of these studies, they showed 4 distinct soil profiles for the Adapazari region in Figure 4 [Sancio et al., 2002].

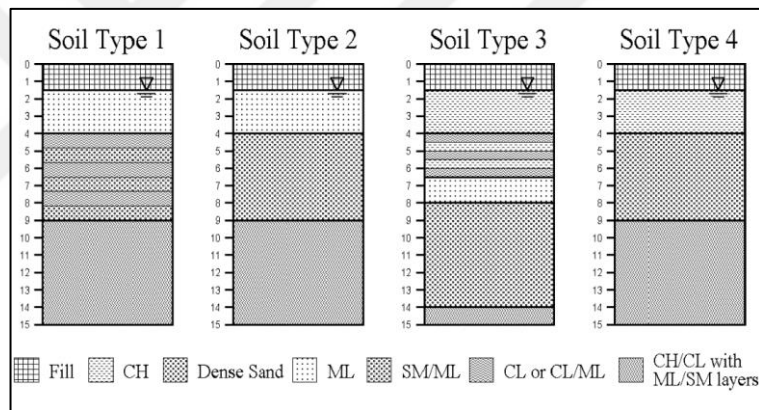


Figure 4.5: Generalized subsurface soil profiles in Adapazari.

The groundwater level of region is shallow and located approximately 1-2 m below the surface and may change depending on the weather conditions [Sancio et al., 2002]. Soil type 1 consists of loose non-plastic silt and sandy silt soils up to 4 meters, and beneath low plasticity clays and medium dense to dense silt to sandy silt soils and interbedded clays, silts and sands are found deeper than 9 m. Soil type 2 is similar to that of Soil type 1, except under loose silt there is dense sand to a depth of about 9 meters. Soil type 3 consists of highly plastic silty clay between 1.5 and 4 meters underlain by interspersed lenses and layers of low to highly plastic silty clay and clayey silt soils. Soil type 4 is similar to that of Soil type 2, except loose silt in soil type 2 is

replaced by medium to high plasticity silty clay soil for 1.5 - 4 meters [Sancio et al., 2002].

Bol et al., (2019) analyzed estimation of undrained shear strength based on CPTu results for Adapazarı region. They conducted many CPTu and laboratory experiments. Based on the extensive CPTu test results provided by Bol et al. (2019), the soil classification was determined based on Schneider et al., (2008). In this context, pore pressure ratio ( $B_q$ ) and net normalized cone resistance ( $Q_t$ ) values were obtained with the CPTu data provided by Bol et al., (2019). These data are superimposed into the chart of Schneider et al., (2008) (Figure 4.5). It is seen that Adapazarı soil which is fluvial deposits transported through Sakarya River (Figures 4.1 and 4.3) falls in Region 1a (Silts and Low  $I_r$  Clays) Region 2 (Sands) and Region 3 (Transitional Soils). Even though the soil behavior type cover three distinct regions, the majority of the data falls in Transitional Soil zone (such as clayey silts, silty clays and silts).

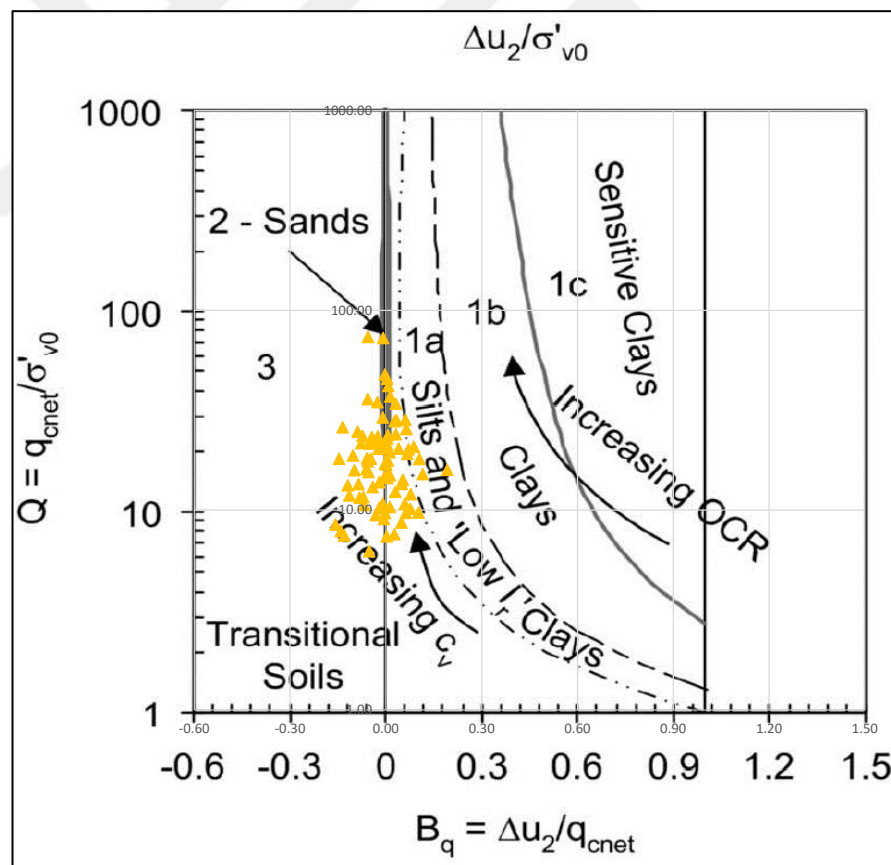


Figure 4.6: Soil behaviour type of Adapazarı Region based on Schneider et al. (2008).

## 5. SPT and CPTu CORRELATIONS

There have been various studies performed on the SPT and CPTu correlations. SPT is among the most preferred tests in the world due to its advantages such as availability and low cost. However, there are repeatability and reliability problems for SPT [Robertson and Cabal, 2014]. Due to its widespread use, SPT has been used in site characterisation studies as a standard practice. The normalized SPT blow count is used to estimate the physical and mechanical properties of the soil and used in the design. CPTu is also used to characterize the in-situ soil properties. CPTu provides continuous data recording along the subsurface profile and the repeatability is more reliable compared to that of SPT. On the other hand, disturbed soil samples can be collected by SPT. Therefore, both SPT and CPTu are used together for geotechnical site investigation projects to construct the idealized soil profile of the site. Consequently, the use of both CPTu and SPT in a soil investigation improves the quality of the subsurface profile and reduces the margin of error [Erol and Çekinmez, 2014]. Therefore, various CPTu-SPT correlations have been developed. Considerable number of studies were performed to correlate SPT blow counts ( $N$ ) and corrected SPT blow counts ( $N_{60}$ ) with CPTu tip resistance ( $q_c$ ). Estimating  $N$  and  $N_{60}$  values as a function of  $q_c$  suggested by De Alencar Velloso (1959) and Meigh and Nixon (1961) in the 1960s. Various researchers proposed number of equations were summarized in Table 5.1.

Table 5.1: Correlations Based on  $q_c$ - $N$  Relationship.

Reference	Soil Properties	Relationship
(De Alencar Velloso 1959)	Clay and silty clay	$q_c / N = 0.35$
	Sandy clay and silty sand	$q_c / N = 0.2$
	Sandy silt	$q_c / N = 0.35$
	Fine sand	$q_c / N = 0.6$
	Sand	$q_c / N = 1.00$
(Meigh and Nixon 1961)	Coarse sand	$q_c / N = 0.2$
	Gravelly sand	$q_c / N = 0.3-0.4$
(Franki Piles 1960) from (Akca 2003)	Sand	$q_c / N = 1.00$
	Clayey sand	$q_c / N = 0.6$
	Silty sand	$q_c / N = 0.5$
	Sandy clay	$q_c / N = 0.4$
	Silty clay	$q_c / N = 0.3$
	Clays	$q_c / N = 0.2$

Table 5.1: Continue.

Schmertmann 1970)	Silt, sandy silt and silt-sand mix.	$([q_c+f_s]/N) = 0.2$
	Fine to medium sand, silty sand	$([q_c+f_s]/N) = 0.3-0.4$
	Coarse sand, sand with gravel	$([q_c+f_s]/N) = 0.5-0.6$
	Sandy gravel and gravel	$([q_c+f_s]/N) = 0.8-1.0$
(Barata et al., 1978)	Sandy silty clay	$(q_c/N)^* = 1.5-2.5$
	Clayey silty sand	$(q_c/N)^* = 2.0-3.5$
(Ajayi & Balogun 1988)	Lateritic sandy clay	$(q_c/N)^* = 3.2$
	Residual sandy clay	$(q_c/N)^* = 4.2$
(Chang 1988)	Sandy clayey silt	$(q_c/N)^* = 2.1$
	Clayey silt, sandy clayey silt	$(q_c/N)^* = 1.8$
(Danziger & de Valleso 1995) * $q_c/N$ (bar/30cm)	Silt, sandy silt and silt-sand	$([q_c+f_s]/N) = 0.2$
	Fine to medium sand, silty sand	$([q_c+f_s]/N) = 0.3-0.4$
	Coarse sand, sand with gravel	$([q_c+f_s]/N) = 0.5-0.6$
	Sandy gravel and gravel	$([q_c+f_s]/N) = 0.8-1.0$
	Silty sand	$(q_c/N)^* = 7.0$
(Danziger et al.,1998) * $q_c/N$ (bar/30cm)	Sand	$(q_c/N)^* = 5.7$
	Silty sand, Silty clay	$(q_c/N)^* = 5.0-6.4$
	Clayey silt	$(q_c/N)^* = 3.1$
	Clay, silt and sand mixtures	$(q_c/N)^* = 1.0-3.5$
	Clayey sand and silty clay	$(q_c/N)^* = 4.6-5.3$
	Sandy clay	$(q_c/N)^* = 1.8-3.5$
(Akca 2003)	Sand	$q_c/N = 0.77$
	Silty sand	$q_c/N = 0.70$
	Sandy silt	$q_c/N = 0.58$
(Alam et al., 2018)	Silty Sand	$q_c = 0.427N$
	Sandy Silt	$q_c = 0.337N$
	Silty Clay	$q_c = 0.319N$
	Lean Clay	$q_c = 0.291N$
(Aşçı et al., 2015)	Silty clay	$q_c = 233.2\exp(1.122N) + 0.4513\exp(0.02096N)$
	Clayey silt	$q_c = 1.228\exp(0.03473N) + 0.3193\exp(0.05133N)$
	Clay	$q_c = 233.2\exp(-1.122N) + 0.4513\exp(0.02096N)$
	Sandy silt	$q_c = 7.187\exp(-0.4827N) + 1.938\exp(0.00989N)$
(Hore et al., 2018)	Sand	$q_c = 1.5538N_{60}^{0.31}$
	Silt	$q_c = 0.3373N_{60}^{0.6284}$
	Clay	$q_c = 0.5637N_{60}^{0.3447}$
	Combined sample (Sand, Silt and Clay)	$q_c = 0.553N_{60}^{0.5556}$
(Jarushi 2015)	Silty Fine Sand	$q_c = 0.12N + 5.0$
	Fine Sand	$q_c = 0.291N + 2.43$
	Fine Sand with Silt	$q_c = 0.15N + 7.2$
	Clayey Fine Sand	$q_c = 4.1N^{0.17}$
	Silty Clayey Fine Sand	$q_c = 0.95N^{0.64}$

Table 5.1: Continue.

(Kara and Gündüz 2010)	Clay	$q_c = 0.1994N^{0.8535}$
	Silt	$q_c = 0.3755N^{0.7342}$
	Sand	$q_c = 0.5334N^{0.809}$
	All	$q_c = 0.1877N^{0.9894}$
(Shahri et al., 2014)	Silty Sand	$q_c = 0.282N^{1.212}$
	Clay	$q_c = 0.409N^{0.779}$
	Sandy silt	$q_c = 0.563N-0.366$
	Sand	$q_c = 0.605N-0.842$
	Gravelly sand to sand	$q_c = 0.3975N^{1.13}$
Ramaswamy et al., (1982)	Sand	$q_c/N = 0.50-0.70$
Ahmed et al., (2014)	Clean sands to sandy silts	$q_c/N = 0.508$
Zhao and Cai (2015)	Silt	$N = 2.089 q_c + 1.485$
	Silty sand	$N = 1.384 q_c + 9.063$
Mohamed and Vanapalli (2015)	Sand	$q_c = 0.533 (N_1)_{60}^{0.8019}$
Costa et al., (2016)	Silty sand	$(q_c/N_{60}) = 0.39$
Aral and Güneş (2017)	CH clay	$q_c = 0.1114 N_{60} + 0.9417$
	CI clay	$q_c = 0.1126 N_{60} + 1.2973$
	SC, SM and SP	$q_c = 0.3892 N_{60} + 2.427$

$q_c/N$  in MPa

\* $q_c/N$  in bar per blow 0.3m

Schmertmann (1978) and Kovacs et al., (1981) stated that the SPT N value is affected by the amount of energy transferred to the rod. Moreover, Douglas and Olsen (1981) showed that soil density and hammer type affect the  $q_c/N$  ratio. In addition, Kasım et al. (1986) stated that permeability and compressibility affect the  $q_c/N$  ratio in sandy soils [Jarushi et al., 2015]

Robertson et al. (1983) suggested a correlation between the ratio of  $(q_c/p_a)/N_{60}$  is a function of mean grain size ( $D_{50}$ ) where the  $D_{50}$  value ranges from 0.001 mm to 1.0 mm (Figure 5.1). In addition, the atmospheric pressure, whose  $q_c$  value is in the same unit, is divided by  $P_a$ , and therefore, it becomes unit less. The ratio of  $(q_c/p_a)/N_{60}$  increases while the grain size increases (Figure 5.1)

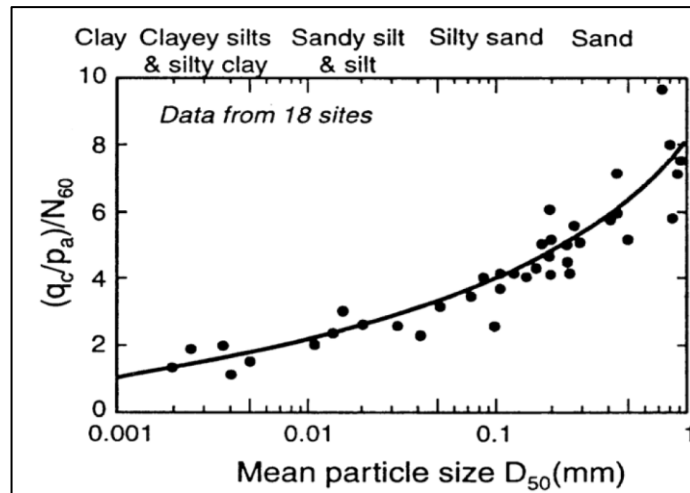


Figure 5.1: CPT-SPT correlations with mean grain size.

Soil grain properties can be obtained from CPTu results using soil behaviour type charts. Robertson et al., (1986) suggest a ratio of  $(q_c/p_a)/N_{60}$  for each soil type region. SBT and a  $(q_c/p_a)/N_{60}$  ratio are shown in Table 5.2 [Robertson and Cabal, 2014]. Using the CPT data, the values in this table the SPT  $N_{60}$  values can be estimated.

Table 5.2: Suggested  $(q_c/P_a)/N_{60}$  ratios.

Zone	Soil Behaviour Type (SBT)	$\frac{(q_c/p_a)}{N_{60}}$
1	Sensitive fine grained	2.0
2	Organic soils – clay	1.0
3	Clays: clay to silty clay	1.5
4	Silt mixtures: clayey silt & silty clay	2.0
5	Sand mixtures: silty sand to sandy silt	3.0
6	Sands: clean sands to silty sands	5.0
7	Dense sand to gravelly sand	6.0
8	Very stiff sand to clayey sand*	5.0
9	Very stiff fine-grained*	1.0

Kulhawy and Mayne (1990)  $(q_c/p_a)/N$  ratio as a function  $D_{50}$  using an extensive database (Figure 5.2). Proposed equations on estimating  $q_c/N$  ratios were summarized in Table 5.3.

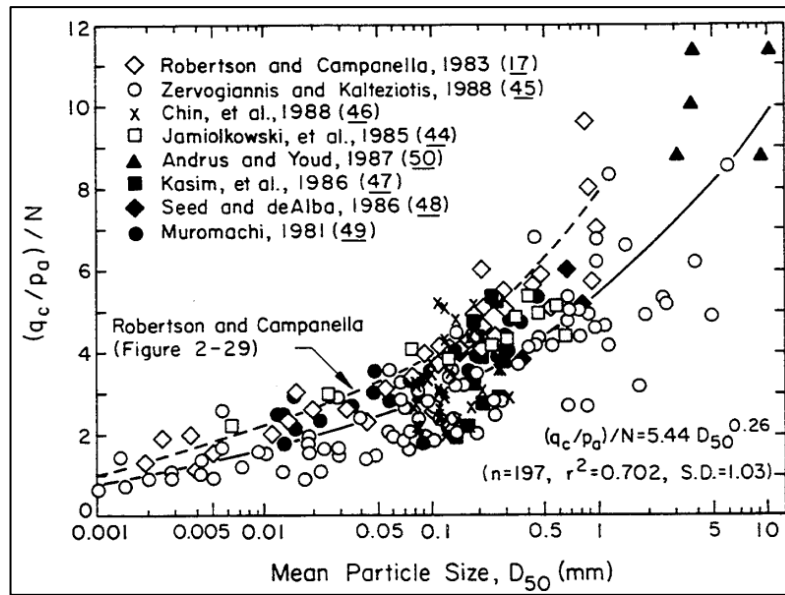


Figure 5.2: CPT-SPT correlation based on grain size.

Table 5.3: Correlations Based on Mean Grain Size, D50.

Reference	Relationship
Kulhawy and Mayne (1990)	$(q_c/P_a)/N = 5.44(D_{50})^{0.26}$
Emrem and Durgunoglu (2000)	$(q_c/N) = \text{func}(D_{50})$

Various studies attempted to analyse possible correlations between the fines content (FC) and the  $q_c/N$  ratio are shown in Table 5.4. In addition, various studies related to fine content are given in Figure 5.3. Figure 5.3 [Kulhawy and Mayne 1990]

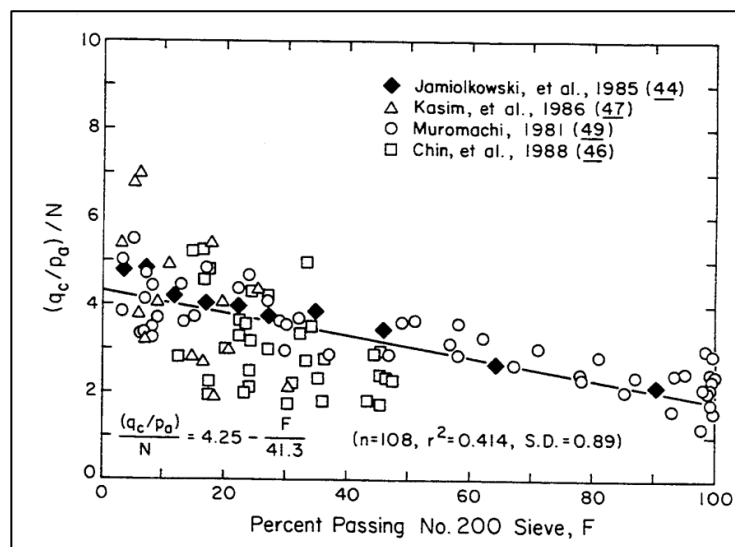


Figure 5.3: CPT-SPT correlation based on fine content.

Table 5.4: Correlations Based on Fines Content, FC%.

Reference	Relationship
Chin et al. (1988)	$(q_c/Pa)/N_{55} = 4.70 - FC/20$
Kulhawy and Mayne (1990)	$(q_c/Pa)/N = 4.25 - FC/41.3$

There are also studies involving the correlations between soil behaviour type index ( $I_c$ ) and  $q_c$ . Jeffries and Davies (1993) proposed a relationship between soil behaviour type index ( $I_c$ ) and SPT and CPTu correlations (Table 5.5). Jeffries and Davies (1993) suggested that SPT  $N_{60}$  values provide better results than SPT  $N$  values due to the insufficient reproducibility of SPT [Robertson and Cabal, 2014].

Robertson (2012) offered an update to the Jeffries and Davies (1993) correlation (Figure 5.4 and Table 5.5).

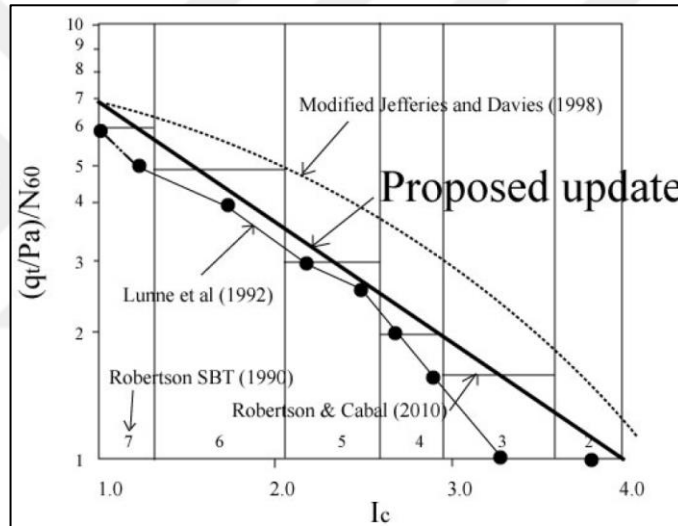


Figure 5.4: SPT-CPT correlations in terms of  $(q_t/P_a)/N_{60}$  and CPT-based SBT index  $I_c$ .

Table 5.5: Correlations Based on Soil Behaviour Type Index,  $I_c$ .

Reference	Relationship
Jeffries and Davies (1993)	$(q_t/P_a)/N_{60} = 8.5(1-I_c/4.6)$
Lunne et al (1997)	$(q_t/P_a)/N_{60} = 8.5(1-I_c/4.6)$
Robertson (2012)	$(q_t/P_a)/N_{60} = 10^{(1.1268-0.2817I_c)}$

## **6. EVALUATION of CPT<sub>u</sub> – SPT N DATABASE of SECTION 6 of THE KMO**

A total of 228 SPT boreholes were drilled and a total of 216 CPT<sub>u</sub> soundings were performed to determine the geological-geotechnical features for the Section 6 of the KMO. In addition, a comprehensive laboratory testing program was carried out to quantify physical and mechanical properties.

The results of a typical SPT profile and a CPT<sub>u</sub> profile are provided in Figure (6.1) and (6.2), respectively.





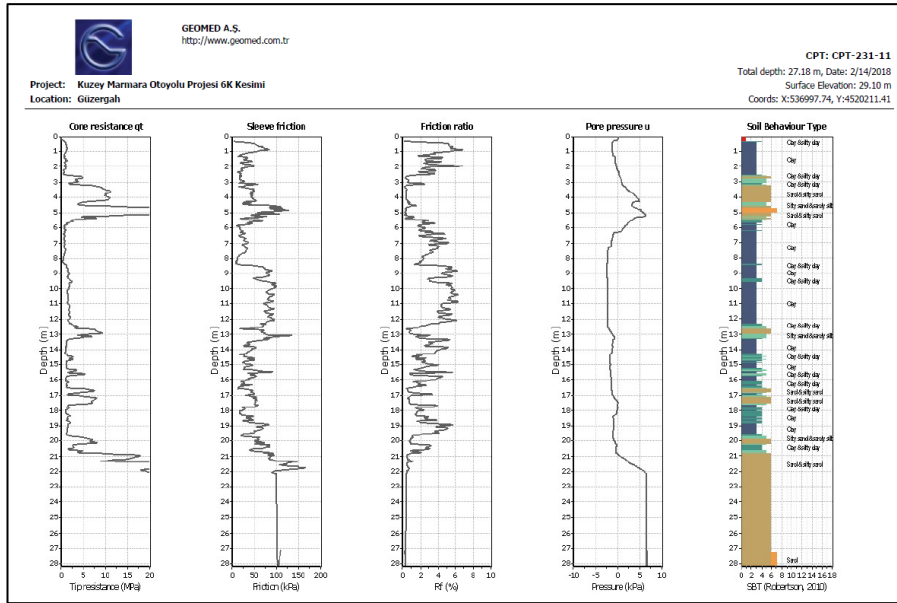


Figure 6.2: A typical CPTu data report.

The Section 6 alignment was divided into a total of 127 sections to manage the subsurface investigation data base (Figure 6.3). In these sections SPT borings and CPTu soundings which are adjacent to each other were matched to create SPT  $N - q_c$  data base. The subsurface investigation program at the sections 89 and 87 along with the entire Region 6 alignment are found in Figures 6.4 and 6.5, respectively. In this way, a total of 76 SPT borings and CPTu soundings which were performed adjacent to each other were matched for the entire Region 6 alignment. All data for the matching SPT – CPTu pairs were provided in Appendix A.



Figure 6.3: Sections 87 through 90.

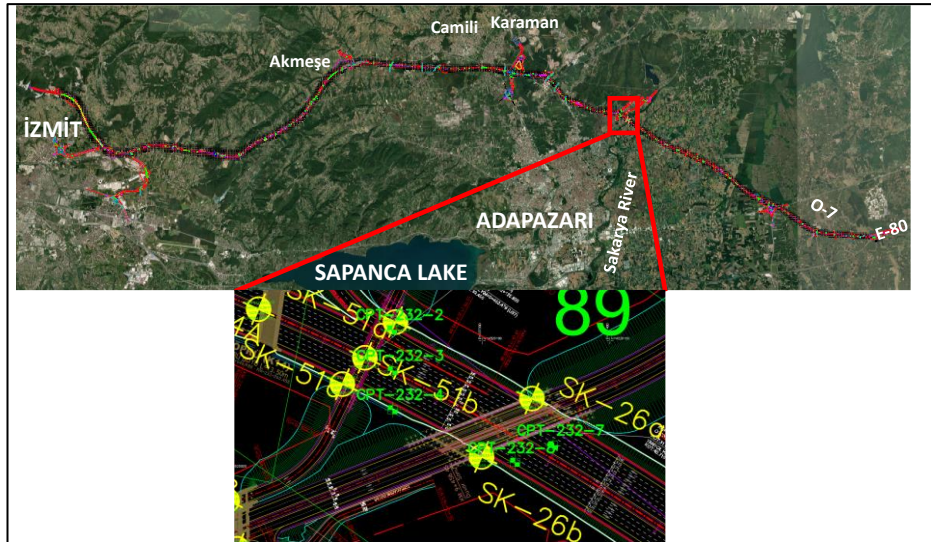


Figure 6.4: Aerial view of the alignment and locations of SPT borings and CPTu soundings at the section 89.

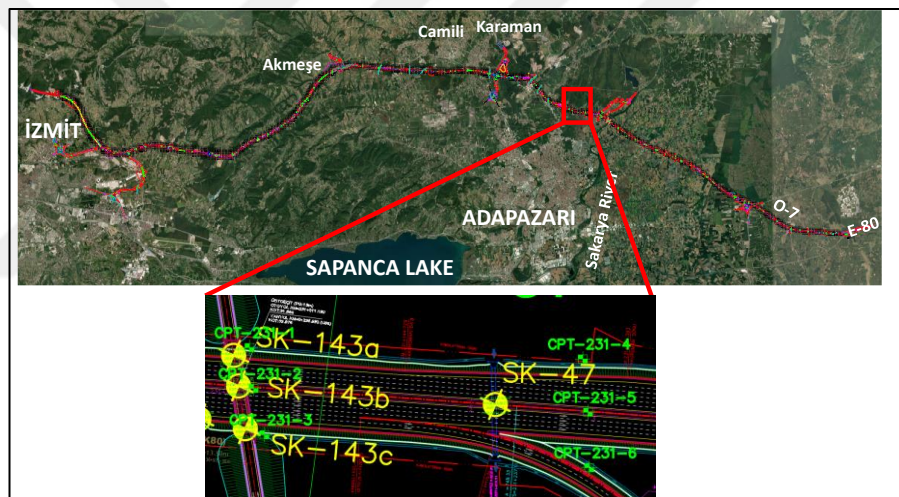


Figure 6.5: Aerial view of the alignment and locations of SPT borings and CPTu soundings at the section 87.

SPT split-spoon sample represent a soil column of 45 cm. On the other hand, tip resistance, friction resistance and dynamic pore water pressure values are obtained at 2 cm intervals in the CPTu soundings. Therefore, data collected by CPTu ( $q_c$ ,  $u_2$ ,  $f_s$ ) and calculated values based on collected data ( $q_t$ ,  $Q_t$ ,  $R_f$ ,  $F_r$ ) were averaged for a distance of 45 cm along the elevations that matched with the respected SPT blow count.

When the entire alignment was examined, a total of 76 SPT borings and CPTu soundings which were performed adjacent to each other were identified. There were a total of 1026 SPT-N and CPTu data pairs were obtained in these SPT-CPTu pairs.

SPT-N values which were recorded blow counts higher than 50 (refusal) were eliminated from the data base. Soil behaviour type index values,  $I_c$ , higher than 2.60 are classified as clayey silt to silty clay and silty clay to clay (fine grained soils) [Robertson, 1990]. Since the aim of this study is to correlate SPT-CPTu for fine grained soils, the entire CPTu data points which has  $I_c$  of 1.31 to 2.60 (coarse grained soils) [Robertson, 1990] were also not included in the data base. Typically, fine grained soils exhibit  $q_c$  of less than 5 MPa and  $Q_t$  of less than 20 [Robertson and Cabal, 2014]. Therefore, the values higher than those limits were also eliminated from the dataset. At the end of this filtering effort, a total of 646 SPT-N and CPTu data pairs were obtained. All these data were provided in Appendix A.

A typical CPTu results ( $q_c$  vs. elevation,  $f_s$  vs. elevation and  $u_2$  vs. elevation) along with the SPT N values for the boring performed adjacent to the CPTu are shown in the Figure 6.6 and Figure 6.7. These graphs are made for all CPTu soundings and SPT borings which were performed adjacent to each other provided in Appendix B.

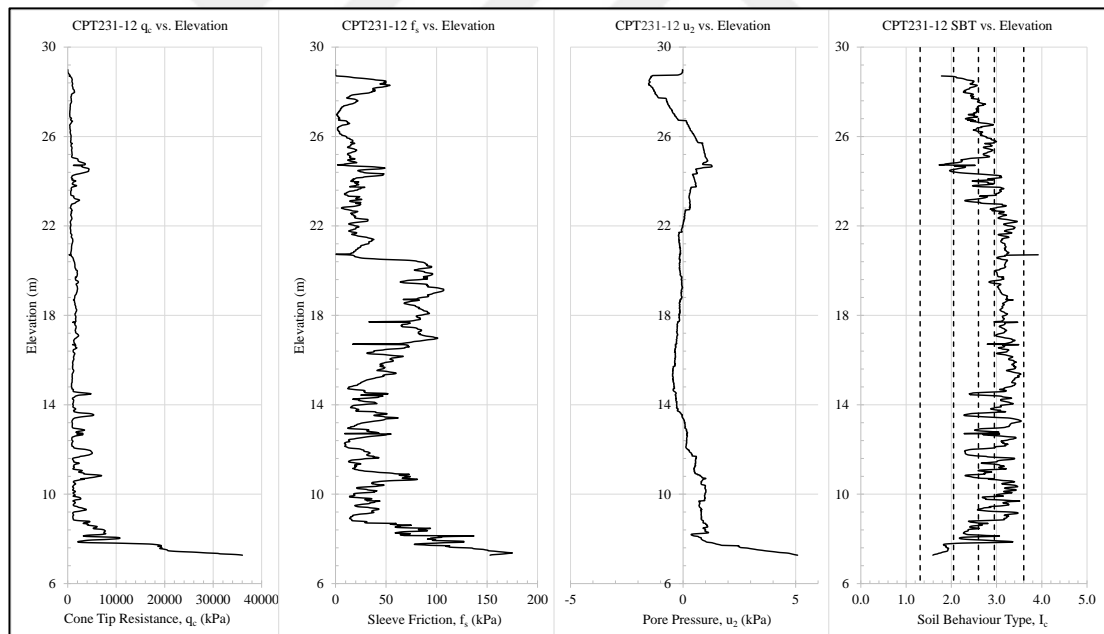


Figure 6.6: A typical CPTu data versus elevation.

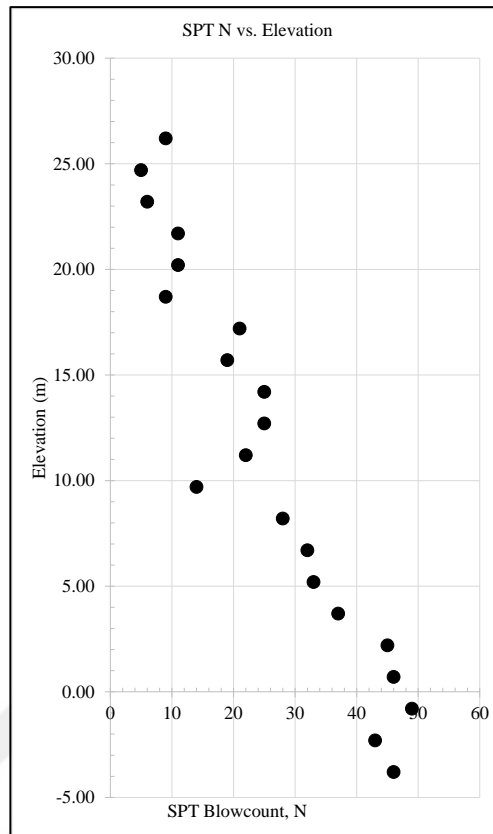


Figure 6.7: A typical SPT data versus elevation.

## 6.1. Soil Behaviour Type

SBT index versus elevations graphs were created for entire CPTu profiles. An example of typical SBT based on Robertson (1990) can be found in Figure 6.8. All SBT graphs are also included in Appendix B. These graphs are divided into sections according to the  $I_c$  ranges indicated in the Figure 3.2. When these graphs were examined, main soil types identified as clayey silt to silty clay and silty clay to clay along the entire route. SBT of a total of 646 SPT-N and CPTu data pairs were given in Figure 6.9. The entire filtered dataset is found to be in Zones 3 (silty clay to clay) and 4 (clayey silt to silty clay) [Robertson, 1990].

In addition to Robertson (1990), the database was also classified according to Schneider et al. (2008). CPTu penetration in sands is fully drained and clays fully undrained, therefore excess pore pressures in sands exhibits a number close to zero and in clays a high positive number. Dense sands and overconsolidated clays exhibit dilative behaviour, therefore, negative pore pressure response under CPTu penetration

is observed. In clayey sands and silts, silty clays and silts in which the CPTu penetration conducted under partial consolidation [Schneider et al., 2008]. In these soils some dissipation of excess pore water pressure develops around advancing cone which results negative shear induced pore pressures adjacent to the cone shaft [Schneider et al., 2008]. The SBT proposed by Robertson (1990) cannot capture this behaviour and Schneider et al. (2008) proposed behavioural classification based on the excess pore pressure response during CPTu penetration. Based on (Schneider et al., 2008), soils can be classified as transitional soil (clayey sands and silts, silty clays and silts) which has partial consolidation during cone penetration (Figure 6.10). The negative or low pore pressure response (negative excess pore pressures) during the CPTu penetration was also indicator of the transient nature of the soil behaviour in the Region 6 alignment (Figure 6.6 and Appendix B).

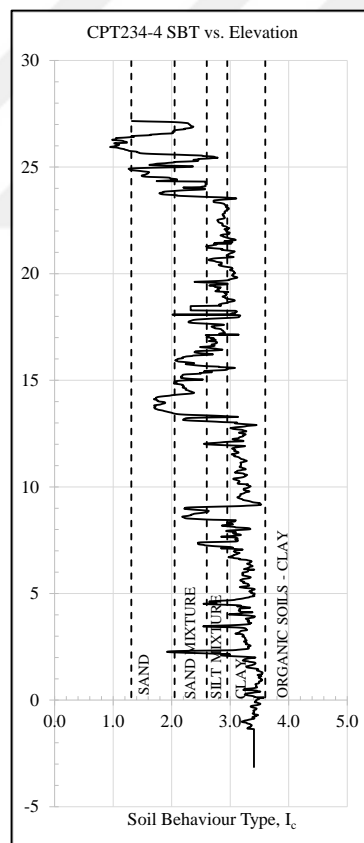


Figure 6.8: A typical SBT index versus elevations graph.

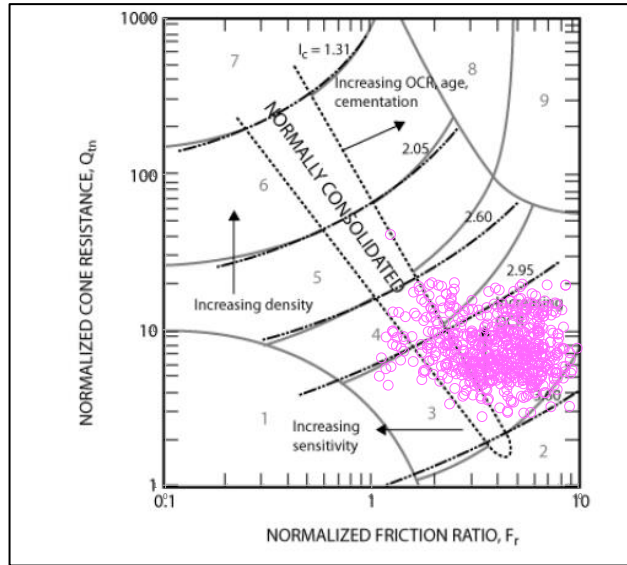


Figure 6.9: KMO data based on Robertson (1990).

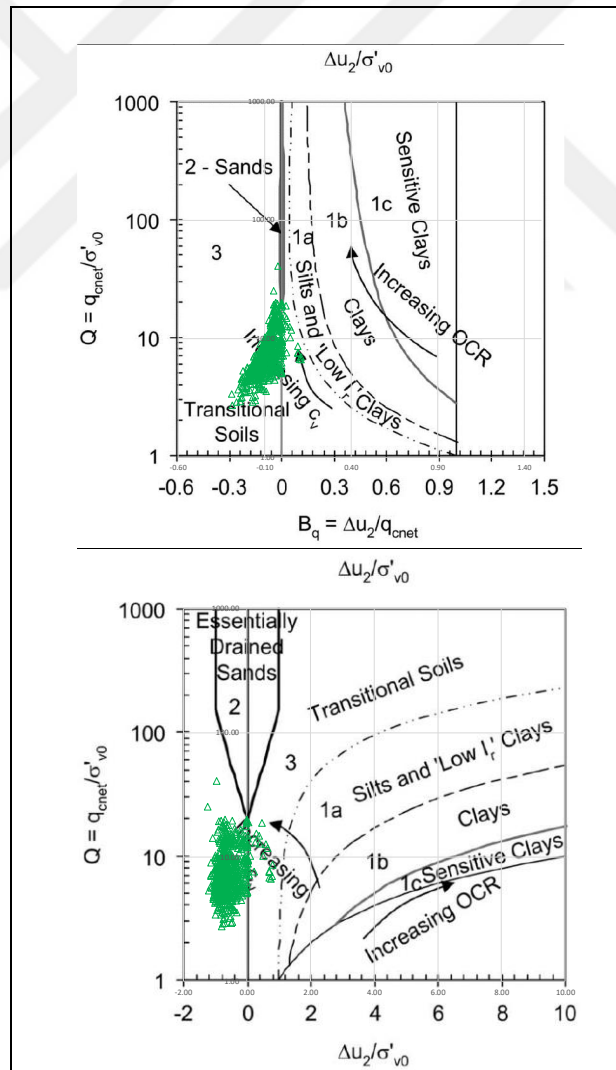


Figure 6.10: KMO data based on Schneider et al. (2008).

## 6.2. Predictive Performances of Previous Studies

The predictive performances of previous studies which were developed for fine grained soils (Table 6.1) were tested with the KMO data.

Table 6.1: The equations selected to be used in this study.

Reference	Soil Types	Relationship
De Alencar Velloso (1959)	Clay and silty clay	$q_c / N = 0.35$
Franki Piles (1960) from Akca (2003)	Clay	$q_c / N = 0.2$
Hore et al., (2018)	Clay	$q_c = 0.5637N_{60}^{0.3447}$
Alam et al., (2018)	Silty clay	$q_c = 0.319N$
Jarushi et al., (2015)	Silty Clayey Fine Sand	$q_c = 0.95N^{0.64}$
Kara and Gündüz (2010)	Clay	$q_c = 0.1994N^{0.8535}$
Shahri et al. (2014)	Clay	$q_c = 0.409N^{0.779}$
Aral and Gunes (2017)	CH clay	$q_c = 0.1114 N_{60} + 0.9417$
Robertson (2012)		$(q_c/Pa)/N_{60} = 10^{(1.1268-0.2817I_c)}$

These equations were applied to SPT and CPTu matching. The calculated  $q_c$  values were compared with the measured ones from the CPTu test results. As a result, the following nine graphs from Figure 6.11 through Figure 6.19 were prepared. 1:1 data line, which represents the perfect match between the measured versus predicted values were given as a reference line along with the best-fit lines in those figures. When estimating  $N_{60}$  from  $N$  values,  $E_R$  at the Equation 2.1 is needed. Sivrikaya and Toğrol (2003) performed a study using comprehensive SPT data base from Turkey and  $E_R$  value of 45 for Turkey was suggested. Therefore, following Sivrikaya and Toğrol (2003),  $E_R$  value of 45 was also used in this study when calculating  $N_{60}$ .

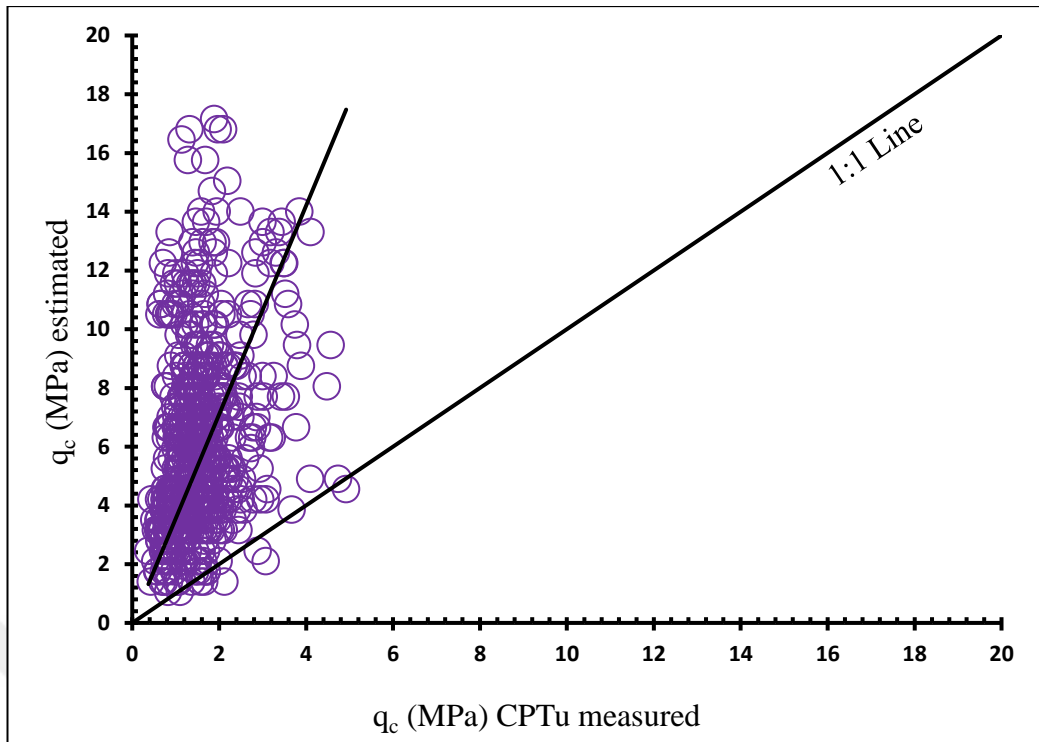


Figure 6.11: De Alencar Velloso (1959) equation versus CPTu data.

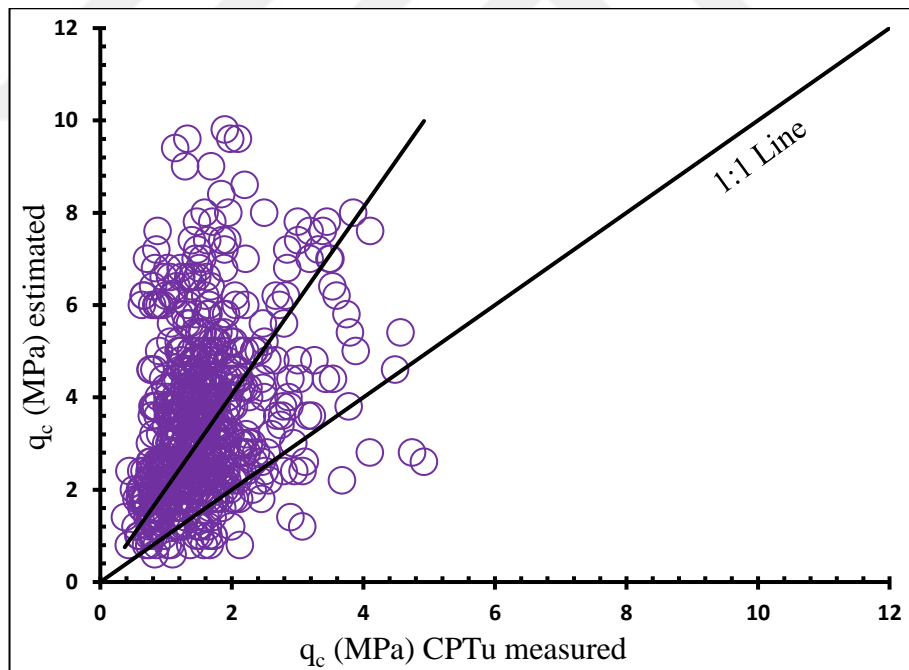


Figure 6.12: Franki Piles (1960) from Akça (2003) equation versus CPTu data.

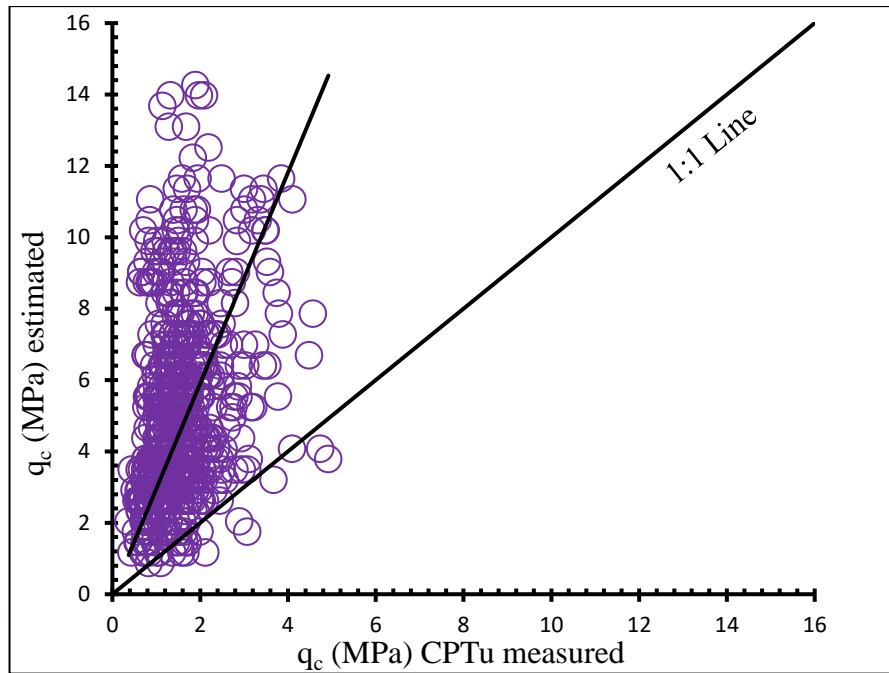


Figure 6.13: Alam et al., (2018) equation versus CPTu data.

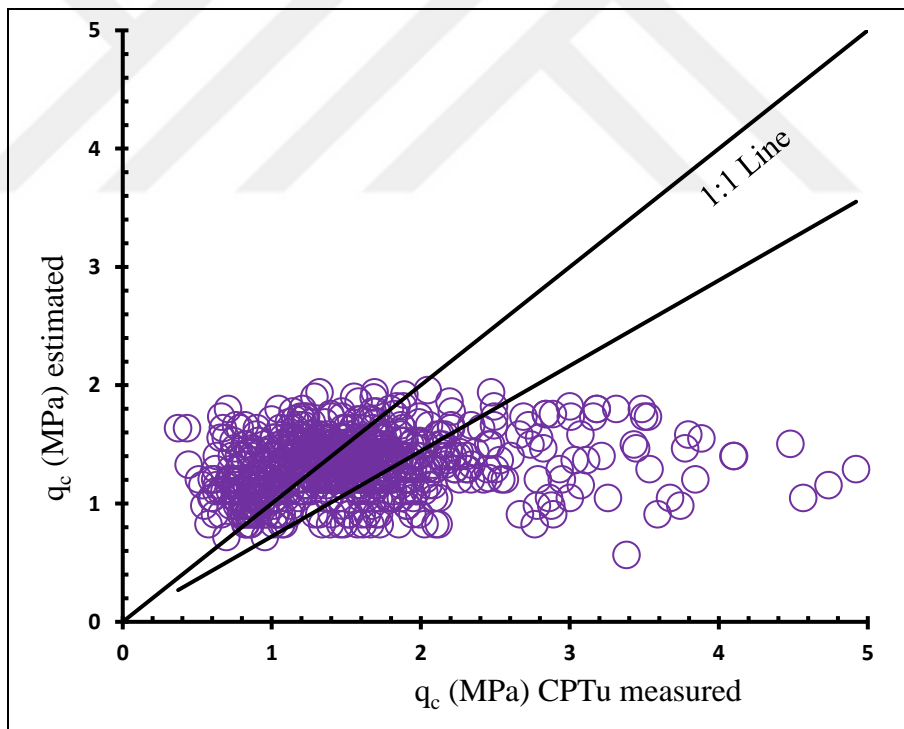


Figure 6.14: Hore et al., (2018) equation versus CPTu data.

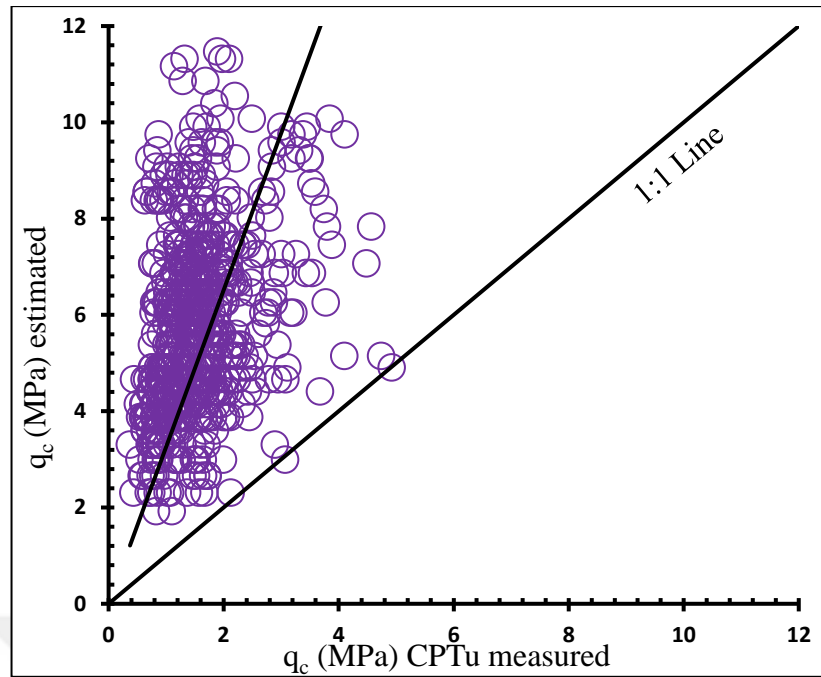


Figure 6.15: Jarushi et al., (2015) equation versus CPTu data.

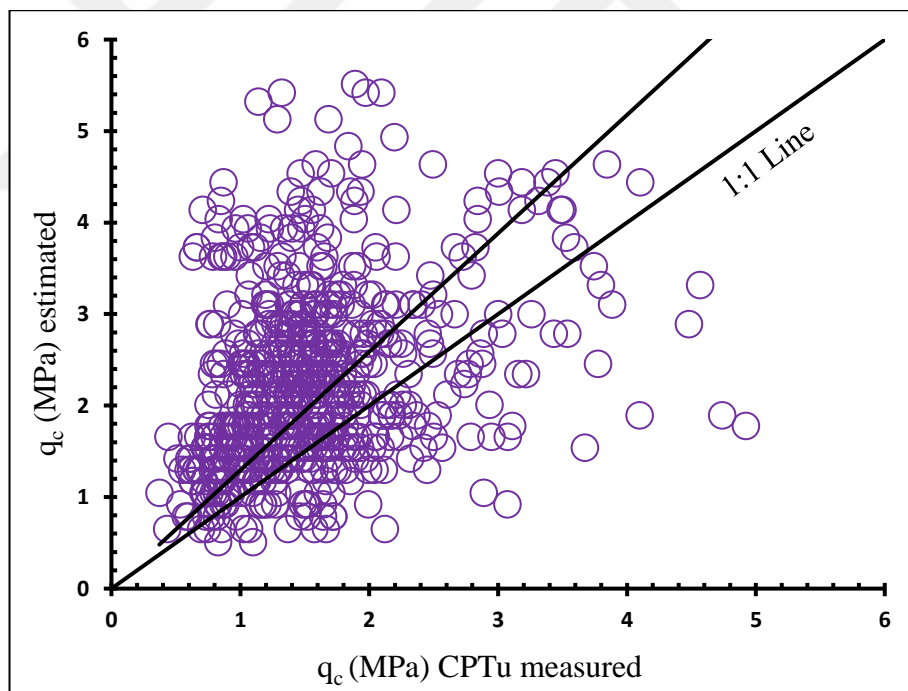


Figure 6.16: Kara and Gündüz (2010) equation versus CPTu data.

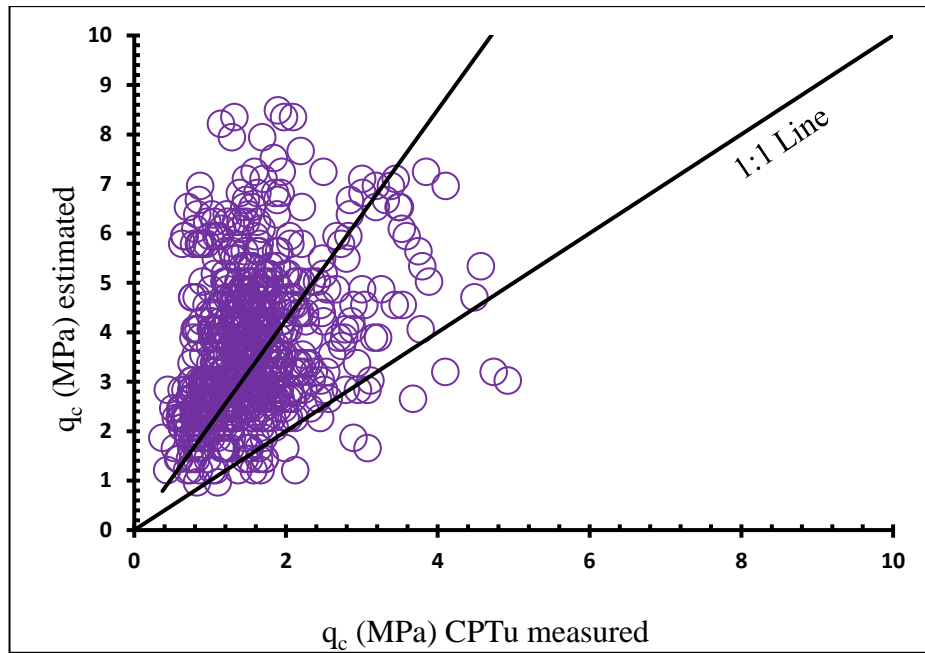


Figure 6.17: Shahri et al., (2014) equation versus CPTu data.

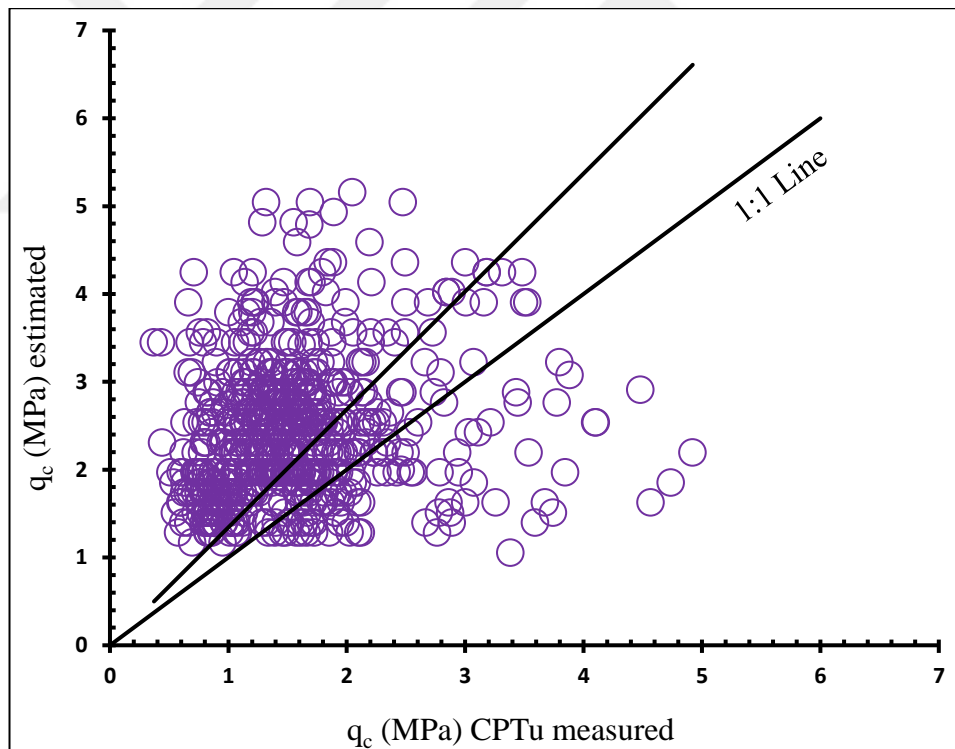


Figure 6.18: Aral and Güneş (2017) equation versus CPTu data.

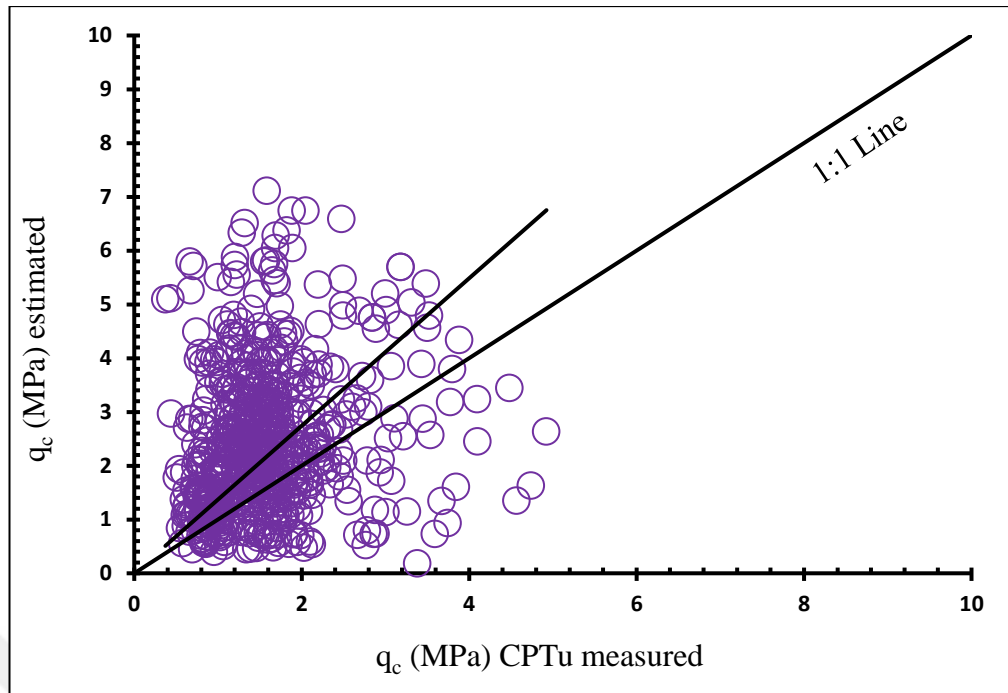


Figure 6.19: Robertson (2012) equation versus CPTu data.

The predictive performances (Figures 6.11 to 6.19) were found poor since they were developed for clays which has fully undrained behaviour under CPTu penetration. The predictive performances of De Alencar Velloso (1959) and Shahri et al., (2014) equations were tested using the CPTu and SPT soundings in the sections 87 and 89. Even though CPTu profiles were high repeatable, the predictive performance of SPT-N values were significantly less than that of measured values in both sections (Figures 6.20 and 6.21).

According to laboratory classification experiments of section 87; water content varied between 18% and 57.1%, percent passing number 200 sieve varied between 17.84% and 98.3%, Liquid limit varied between 38% and 74.24%, Plastic limit varied between 17.38% and 34.52% and Plasticity index varied between 30.87% and 47% for the transient soils. The ground water table located at 1,7 m to 5.5 m below ground surface.

On the other hand, laboratory classification experiments of section 89; water content varied between 19.9% and 57.72%, percent passing number 200 sieve varied between 52.19% and 99.9%, Liquid limit varied between 25.62% and 89.7%, Plastic limit varied between 17.19% and 37% and Plasticity index varied between 14% and 55.3% for the transient soils. The ground water table located at 2 m to 6.5 m below ground surface.

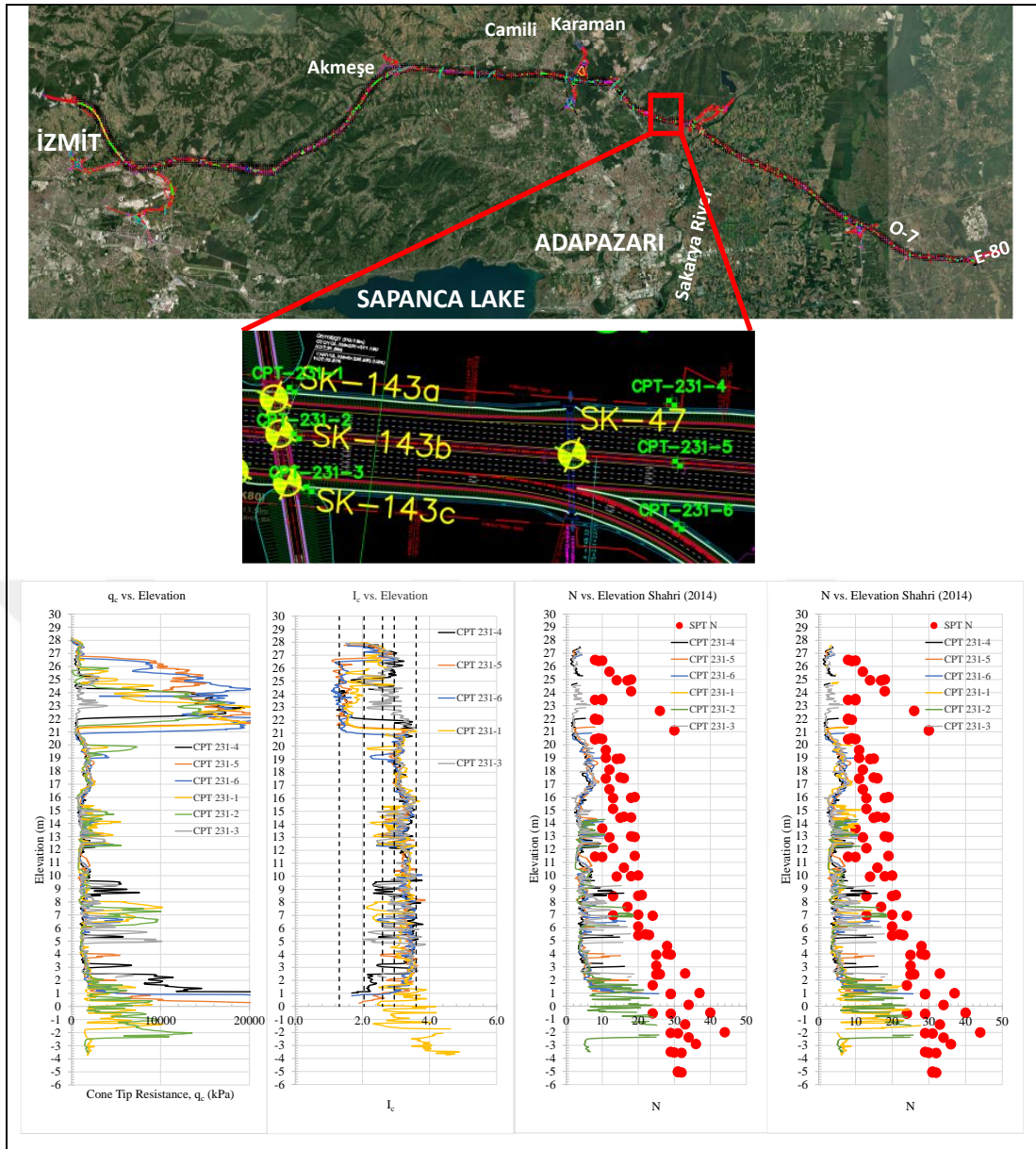


Figure 6.20: Predictive performance of previous works on section 87.

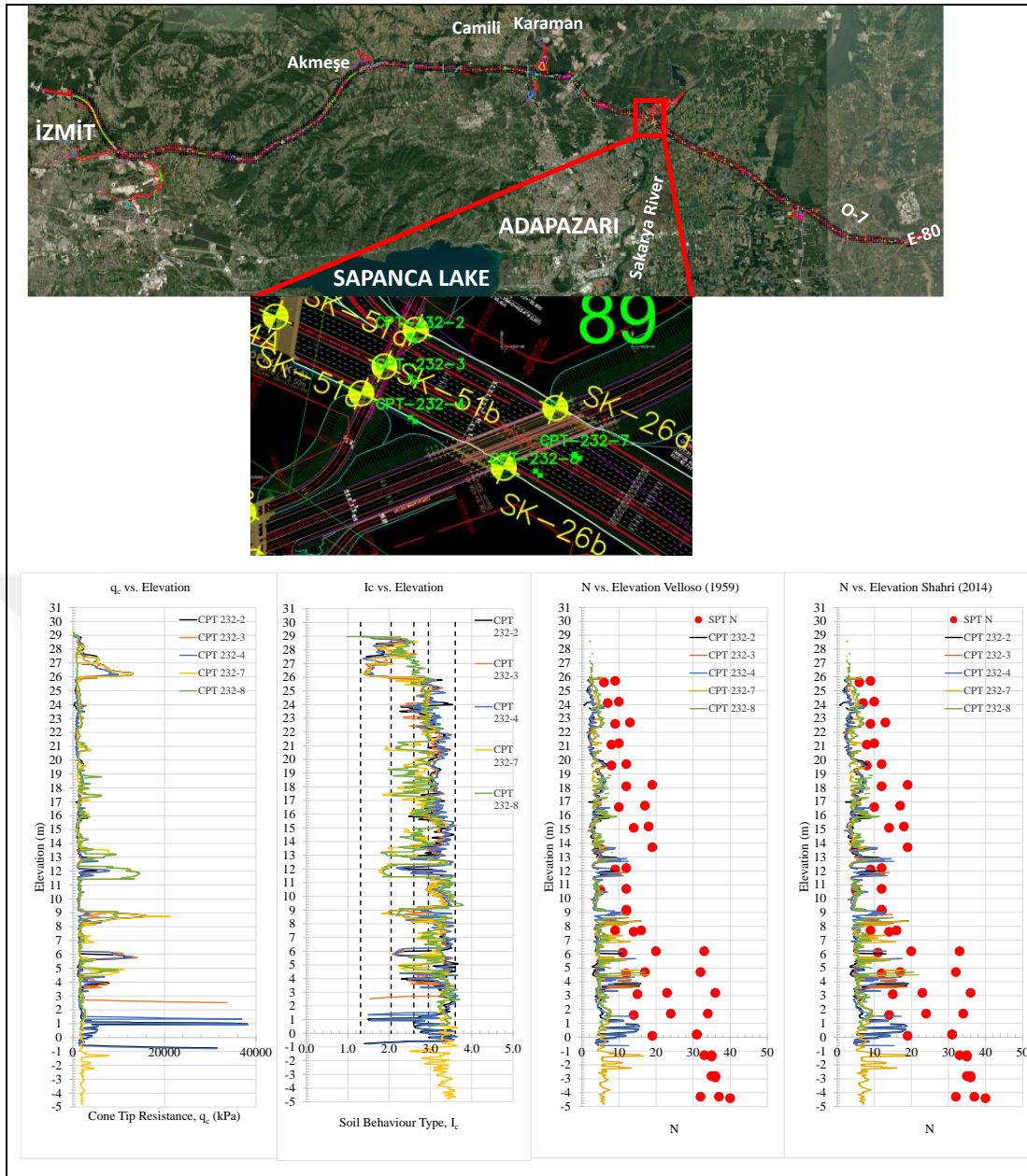


Figure 6.21: Predictive performance of previous works on section 89.

As a result, it is clear that the predictive performances of previous equations were found to be poor. The most important reason for this situation is that the correlations obtained from past studies were for clays which has fully undrained shear behaviour under CPTu penetration. However, the KMO data composed of transitional soil in which CPTu penetration occurs under partial drainage condition according to Schneider et al., (2008). Thus, there is a need for proposing equation for transient soils.

### 6.3. Correlation of This Study

The direct relationship between the CPTu tip resistance and the SPT blow count, which is mostly used in previous studies, is considered.  $q_c/\text{Pa}$  and SPT-N graph obtained from CPTu and SPT field experiments is found in Figure 6.22. In addition,  $q_c/\text{Pa}$  and  $N_{60}$  graph is also created (Figure 6.23). In addition,  $I_c$  and  $q_t/\text{Pa}/N$  graph was also created (Figure 6.24).

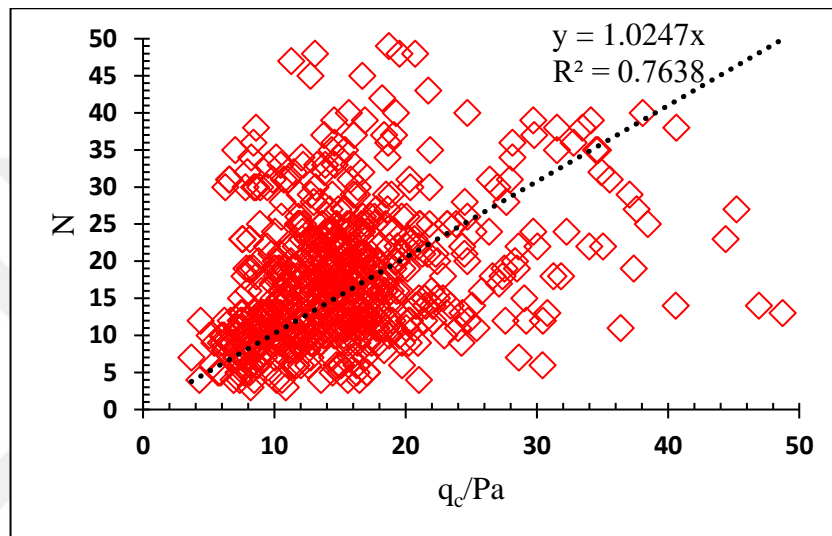


Figure 6.22: SPT-N versus  $q_c/\text{Pa}$  graph.

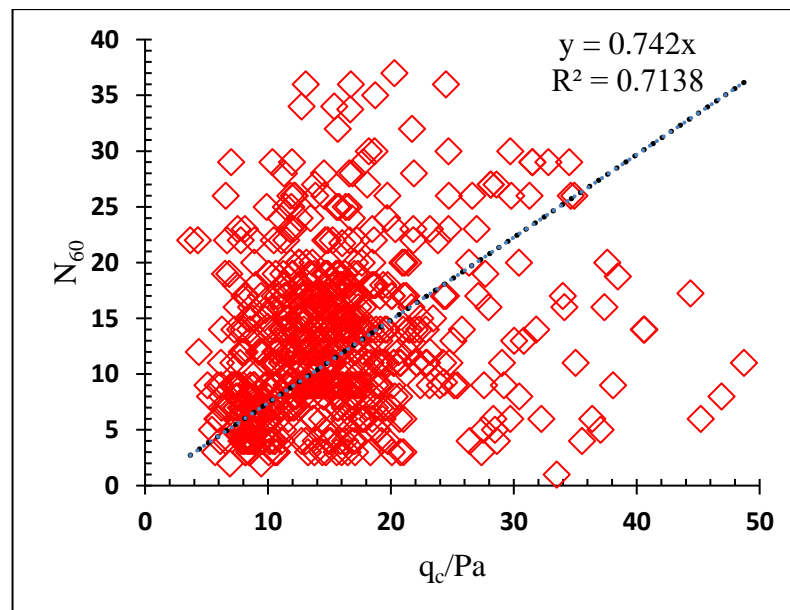


Figure 6.23: SPT- $N_{60}$  versus  $q_c/\text{Pa}$  graph.

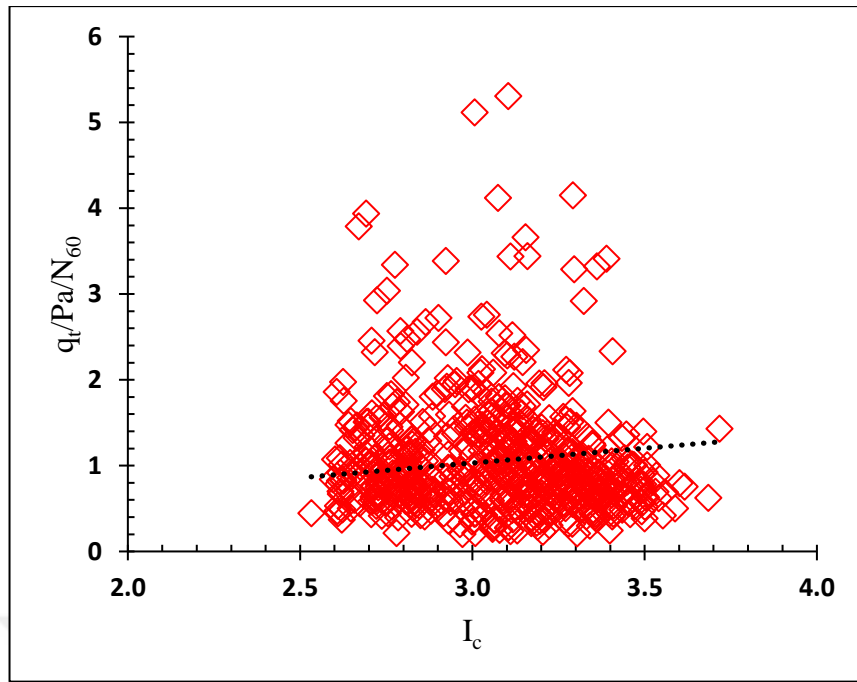


Figure 6.24:  $q_t/P_a/N_{60}$  versus  $I_c$  graph.

The equation and regression values obtained from the  $q_c/P_a$  vs.  $N$  and  $q_c/P_a$  vs.  $N_{60}$  data are shown in the Table 6.2.

SBT index and  $q_t/P_a/N_{60}$  relation of the KMO data is provided in Figure 6.24. As mentioned in the previously  $I_c$  values less than  $I_c$  2.60 are not used in the data base since the aim of the study is to correlate SPT  $N$  with CPTu for fine-grained soil. As can be seen in this graph, data was clustered in a narrow range and a has a poor regression value. Therefore, a correlation equation with the soil behaviour type index for transient soil of the region 6 alignment of the KMO is not recommended.

Table 6.2: The equations proposed in this study.

Proposed Equations of This Study	Regression ( $R^2$ )
$N = q_c/P_a$	0.76
$N_{60} = 0.742q_c/P_a$	0.71

### 6.3.1. Predictive Performance of Proposed Equations

The predictive performance of the first equation in Table 6.2 were analysed in Figures 6.25 and 6.26 for the in-situ testing program conducted at the section 89 and section 87, respectively.

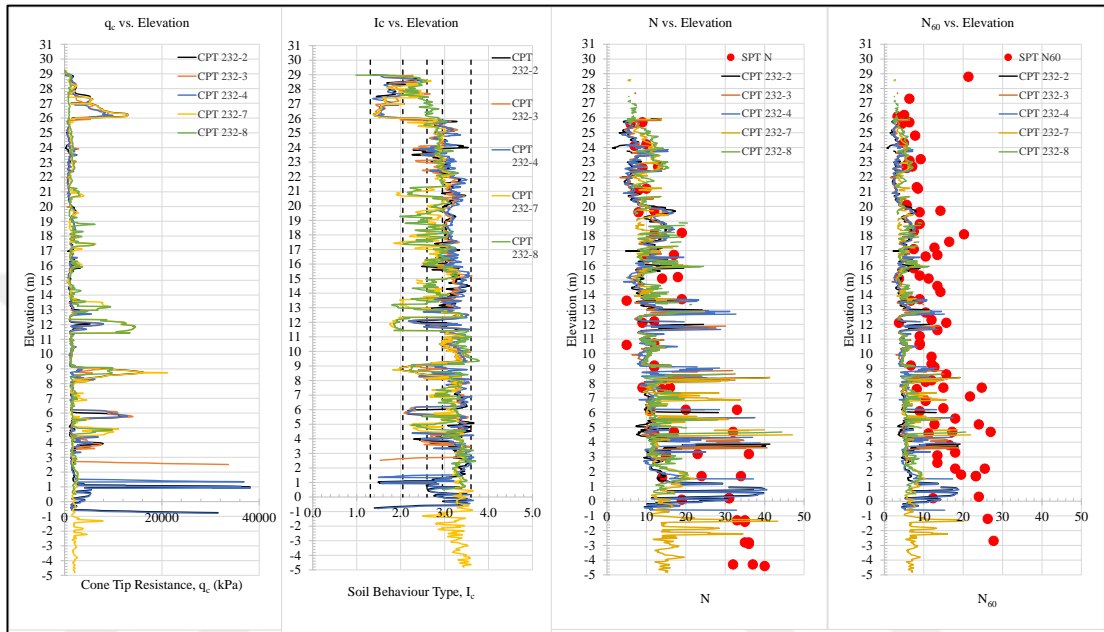


Figure 6.25: Predictive performance of the proposed equations for the sections 89.

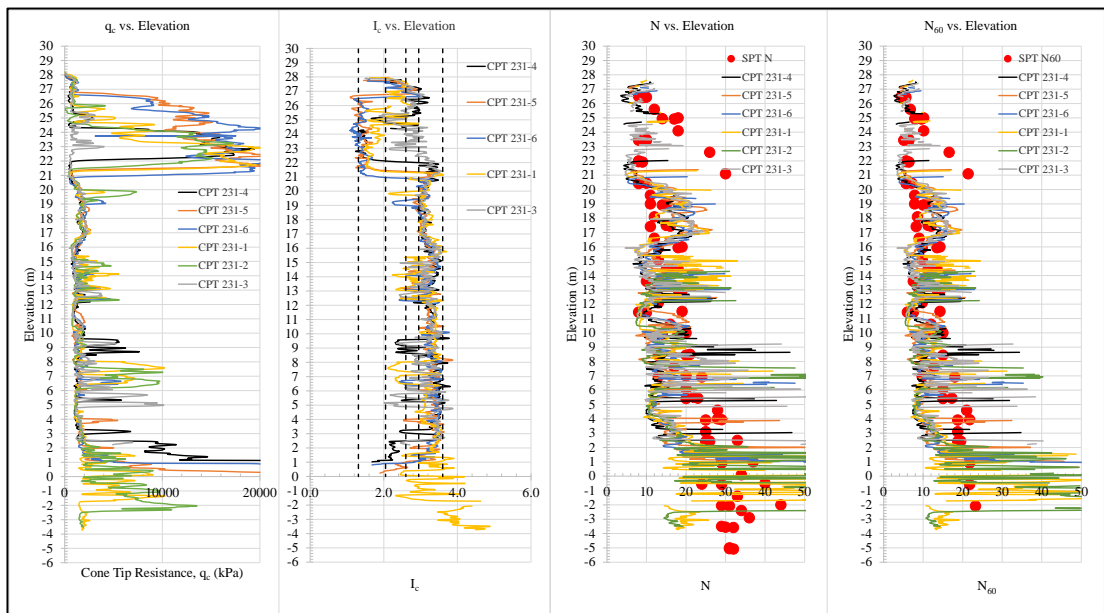


Figure 6.26: Predictive performance of of the proposed equations for the section 87.

Figures 6.25 and 6.26 have shown that the equations proposed in this study to correlate SPT results with CPTu data for transitional soil provided reasonable estimation (Appendix C).



## 7. CONCLUSION

Standard penetration test, SPT, and Piezocone test, CPTu, are commonly used for geotechnical site characterization. These experiments have some advantages and disadvantages. There are concerns about the repeatability of SPT results. In contrast, CPTu provides continuous data logging and is repeatable compared to. However, CPTu is a much more expensive experiment than SPT. Engineers use this test together in geotechnical site investigation projects to create an idealized soil profile from the past to the present.

Within the scope of this study, SPT and CPTu test data made in the project of the 6<sup>th</sup> section of the Northern Marmara Highway (KMO) between Km 223 and Km 251 were used. The soil profile of the site consists of transitional soils such as clayey silts, silty clays and silts. In addition, a literature review was conducted for the estimation of SPT blow counts using CPTu data. In addition, the predictive performances of some equations in the literature along the highway alignment were examined. As a result, the predictive performances of the existing equations in the literature are not suitable to estimate SPT-N values using CPTu data for transitional soils.

The in-situ test results performed by the KMO was used as a case study to establish a correlation for transitional soils. Two separate equations to estimate SPT-N and SPT-N<sub>60</sub> values as a function of  $q_c$  were developed. The performance of these two equations along the highway route is examined in detail. These correlations can be used as a guide for future infrastructure development to be built around the Northern Marmara Motorway (KMO) between Km 223 and Km 251.

## REFERENCES

- Aggour M. S., Radding W. R., (2001), “Research Report: Standard Penetration Test (SPT) Correction, Final Report”, Technical Report No: MD 20742, Department of Civil and Environmental Engineering, University of Maryland College Park, USA.
- Ahmed S. M., Agaiby S. W., Abdel-Rahman A. H., (2014), “A Unified CPT–SPT Correlation for Non-Crushable and Crushable Cohesionless Soils”, *Ain Shams Engineering Journal*, 5(1), 63–73.
- Ajayi L. A., L. A. Balogun., (1988), “Penetration Testing in Tropical Lateritic and Residual Soils – Nigerian Experience”, *Proceedings of the First International Symposium on Penetration Testing*, Vol 1, 315-328.
- Akca N., (2003), “Correlation of SPT–CPT data from the United Arab Emirates”, *Engineering Geology*, 67(3), 219 –231.
- Alam M., Aaqib M., Sadiq S., Mandokhail J. S., Adeel B. M., Rehman M., Kakar A. N., (2018), “Empirical SPT-CPT correlation for soils from Lahore, Pakistan”, 1st International Conference on Advances in Engineering and Technology ,414, Quetta, Pakistan, 2-3 April.
- ASTM, (1998), *Standard Test Method for Mechanical Cone Penetration Tests of Soil*, ASTM D3441-98, American Society for Testing and Materials.
- ASTM, (2011), *Standard Test Method for Performing Electronic Friction Cone and Piezocone Penetration Testing of Soils*, ASTM D1586-11, American Society for Testing and Materials.
- ASTM, (2012), *Standard Test Method for Performing Electronic Friction Cone and Piezocone Penetration Testing of Soils*, ASTM D5778-12, American Society for Testing and Materials.
- ASTM, (2016), *Standard Test Method for Energy Measurement for Dynamic Penetrometers*, ASTM D4633-16, American Society for Testing and Materials.
- ASTM, (2019), *Standard Test Methods for Downhole Seismic Testing*, ASTM D7400-19, American Society for Testing and Materials.
- Aral I. F., Gunes E., (2017), “Correlation of Standard and Cone Penetration Tests: Case Study from Tekirdag (Turkey)”, *IOP Conference Series: Materials Science and Engineering*, 245(3), 032028.
- Aşçı M., Kurtulus C., Kaplanvural I., Mataracioglu M. O., (2015), “Correlation of Spt-Cpt Data From The Subsidence Area in Gölcük, Turkey”, *Soil Mechanics and Foundation Engineering*, 51(6), 268–272.

Barata L. E. S., Baker P. M., Gottlieb O. R., Rùveda E. A., (1978), "Neolignans of *Viola surinamensis*", *Phytochemistry*, 17(4), 783–786.

Begemann H. K. S., (1953), "Improved method of determining resistance to adhesion by sounding through a loose sleeve placed behind the cone", *Proceedings of the 3rd International Conference on Soil Mechanics and Foundation Engineering*, 213-17, Zürich, Switzerland, 16-27 August.

Bol E., (2003), "Adapazari zeminlerinin geoteknik özellikleri", PhD Thesis, Sakarya University.

Bol E., (2013), "The influence of pore pressure gradients in soil classification during piezocone penetration test", *Engineering Geology*, 157, 69–78.

Bol E., Önalp A., Özocak A., Sert S., (2019), "Estimation of the undrained shear strength of Adapazari fine grained soils by cone penetration test", *Engineering Geology* 261(4), 105277.

Bowles J. E., (1988), "Foundation Analysis and Design", 0-07-006776-7, McGraw-Hill Book Company Limited.

Bray J. D., Sancio R. B., Durgunoglu T., Onalp A., Youd L. F., Stewart J. P. C., Seed R. B., Cetin K. O., Bol E., Baturay M. B., Christensen C., Onalp A., Karadayilar T., (2004), "Subsurface Characterization at Ground Failure Sites in Adapazari, Turkey", *J. Geotech. Geoenviron. Eng.*, 130(7), 673-685.

Chang M. F., (1988), "In-situ testing of residual soils in Singapore". *Proceedings 2nd International Conference Geomechanics in Tropical Soils*, 97-108, Singapore, 12-14 December.

Chin C. T., Duann S. W., Kao T. C., (1988), "SPT-CPT correlations for granular soils", *Proceedings of International Symposium on Penetration Testing*, 335-339, Orlando, United States, 20-24 March.

Clayton C. R. I., (1995), "The standard penetration test (SPT) methods and use", 9780860174196, Construction Industry Research and Information Association.

Coduto D. E., (1994), "Foundation Design Principles and Practices", 978-0135897065, Prentice-Hall Inc.

Costa Y. D., Cunha E. S, Costa C. L, (2016), "Correlations between SPT and CPT data for a sedimentary tropical silty sand deposit in Brazil", *Geotechnical and Geophysical Site Characterisation 5*, 407–412, Gold Coast, Queensland, Australia, 5-9 September.

Danziger B. R., Velloso D. A., (1995), "Correlations between the CPT and the SPT for some Brazilian soils", *CPT'95*, 2, 155-159, Linköping, Sweden, 4-5 October.

Danziger F. A. B., Almeida M. S. S., Paiva E. N., L. Mello G. F. S., Danziger B. R., (1998), "The piezocone as a tool for soil stratification and classification". Proc. XI COBRAMSEG, 2, 917-926.

De Alencar Velloso D., (1959) "Oensaio de diepsondeering e a determinacao da capacidade de cargo do solo", Rodovia, 29.

Douglas B. J., Olsen R. S., (1981), "Soil classification using electric cone penetrometer" Symposium on Cone Penetration Testing and Experience. Proceedings of the ASCE National Convention, 209-227, St. Louis, USA, October.

Durgunoğlu H. T., Toğrol E., (1974) "Penetration testing in Turkey: State-of-the-art report", In Proceedings of the European Symposium on Penetration Testing, 137, Stockholm, Sweden, June.

Emrem C., Durgunoglu H. T., (2000), "Türkiye CPT veri tabanı ve mevcut amprik bağlantıları ile karşılaştırma", Zemin Mekanığı ve Temel Mühendisliği Sekizinci Ulusal Kongresi, Istanbul, 26-27 October.

Erol A. O., Çekinmez Z., (2014), "Geoteknik Mühendisliğinde Saha Deneyleri", 14 - 01, Yüksel Proje Yayınları.

Mayne P. W., Christopher B. R., DeJong J., (2002), "Subsurface Investigations (Geotechnical Site Characterization)", Technical Report No: FHWA-NHI-01-031, U.S. Department of Transportation, Federal Highway Administration, USA.

Hore R., Al-Mamun S., Ansary M. A., (2018), "Spt-Cpt Correlations For Reclaimed Areas Of Dhaka", Journal of Engineering Science, 09(1), 35-46.

Jarushi F., AlKaabim S., Cosentino P., (2015), "A New Correlation between SPT and CPT for Various Soils", World Academy of Science, Engineering and Technology International Journal of Geological and Environmental Engineering, 9(2), 101-107.

Jefferies M. G., Davies M. P., (1993), "Use of CPTU to estimate equivalent SPTN<sub>60</sub>", Geotech. Testing Journal, 16(4), 458-468.

Kara O., Gündüz Z., (2010), "Correlation between CPT and SPT in Adapazari, Turkey", 2nd International Symposium on Cone Penetration Testing, 2-18, California, United States, 9 March.

Kasim A. G., Chu Ming-Yau Curtis J. N., (1986), "Field Correlation of Cone and Standard Penetration Tests.", ASCE Journal of Geotechnical Engineering, 112(3), 368- 372.

Komazawa M., Morikawa H., Nakamura K., Akamatsu J., Nishimura K., Sawada S., Erken A., Onalp A., (2002), "Bedrock structure in Adapazari, Turkey-a possible cause of severe damage by the 1999 Kocaeli earthquake", Soil Dynamics and Earthquake Engineering, 22, 829-836.

Kovacs W. D., Salomone L. A., Yokel F. Y., (1981), "Energy measurement in the standard penetration test", Technical Report No: NBS BSS 135, Department of Commerce, National Bureau of Standards, USA.

Kullhawy F. H., Mayne P. H., (1990), "Manual on estimating soil properties for foundation design", Technical Report No: EPRI-EL-6800, Electric Power Research Institute, Cornell University, United States.

Liao S. S. C., Whitman R. V., (1986), "Overburden correction factors for SPT in sand", Journal of geotechnical engineering, 112(3), 373-377.

Lunne T., Robertson R.K., Powell J. J. M., (1997), "Cone penetration testing in geotechnical practice", 0-7514-0393-8 1, E & FN Spon Routledge. McGraw Hill Book Company.

McGregor J. A., Duncan J. M., (1998), "Performance and use of the standard penetration test in geotechnical engineering practice", Technical Report No: 9781118651650, Virginia Polytechnic Institute, Virginia State University, USA.

Meigh A. C., Nixon I. K., (1961), "Comparison of in-situ tests of granular soils", Proceedings of 5th international Conference on Soil Mechanics and Foundation Engineering, 499, Paris, France, 17-22 July.

Mohamed F. M. O., Vanapalli S. K., (2015), "Bearing Capacity of Shallow Foundations in Saturated and Unsaturated Sands From SPT– CPT Correlations", International Journal of Geotechnical Engineering, 9(1), 2–12.

Nixon I. K., (1982), "Standard penetration test. State of the art report.", In Proceedings of the 2nd European Symposium on Penetration Testing, 3-24, Amsterdam, Netherlands, 24-27 May.

Özer A. T., Bartlett S.F., Lawton E. C., (2010), "CPTU for consolidation properties of Lake Bonneville clay", 2nd International Symposium on Cone Penetration Testing, 49-56, Huntington Beach, United States, 9-11 May.

Ramaswamy S. R., Daulah I, U., Hazan Z., (1982), "Pressuremeter Correlations with Standard Penetration Tests", The 2nd European Symposium on Penetration, 137–142, Amsterdam, Netherlands, 24-27 May.

Ramsey N., (2002), "A Calibrated Model for The Interpretation of Cone Penetration Tests (Cpts) In North Sea Quaternary Soils", Offshore Site Investigation and Geotechnics Diversity and Sustainability Proceedings of an International Conference, 341–356, London, United Kingdom, 26-28 November.

Robertson P. K., (1990), "Soil Classification Using the Cone Penetration Test", Canadian Geotechnical Journal, 27(1), 151-158.

Robertson P. K., (1991), "Soil Classification by the Cone Penetration Test" Reply", Canadian Geotechnical Journal, 28(1), 176-178.

Robertson P. K., (2010). "Soil Behaviour Type from the CPT: An Update", 2nd International Symposium on Cone Penetration Testing, 575-583, Huntington Beach, California, USA, 9-11 May.

Robertson P. K., (2012) "Interpretation of in-situ tests – some insights", Proc. 4th Int. Conf. on Geotechnical & Geophysical Site Characterization, 1-22, Recife, Brazil, 17-21 September.

Robertson P. K., Cabal K. L., "(2014), Guide to Cone Penetration Testing for Geotechnical Engineering", 6th Edition, Gregg Drilling & Testing, Inc.

Robertson P. K., Campanella R. G., Gillespie D., and Greig J., (1986), "Use of Piezometer Cone Data", In-Situ 86 Specialty Conference, 1263-1280, Blacksburg, Virginia, USA, 23-25 June.

Robertson P. K., Campanella R. G., Wightman A., (1983), "SPT–CPT Correlations", Journal of Geotechnical Engineering, 109(7), 1449–1459.

Sahahri A., Juhlin C., Malemir A., (2014), "A Reliable Correlation of SPT-CPT Data for Southwest of Sweden", Electronic Journal of Geotechnical Engineering. 19(E), 1013-1032.

Sancio R. B., Bray J. D., Stewart J. P., Youd T. L., Durgunoglu H. T., Onalp A., Seed R. B., Christensen C., Baturay M. B., Karadayilar T., (2002), "Correlation between ground failure and soil condition in Adapazari, Turkey", Soil Dynamics and Earthquake Engineering, 22(9-12), 1093-1102.

Sanglerat G., (1972), "The penetrometer and soil exploration, developments in geotechnical engineering", 0-444-40976-9, Elsevier Publishing Company.

Schmertmann J.H., (1978), "Guidelines for Cone Penetration Test, Performance and Design." Technical Report No: FHWA-TS-78-209, U.S. Department of Transportation, Washington, USA.

Schmertmann J. H., (1970), "Static cone to compute static settlement over sand", In ASCE, Journal of the Soil Mechanics and Foundations Division. 96 (3), 1011-1043.

Schneider J. A., Randolph M. F., Mayne P. W., Ramsey N. R., (2008), "Analysis of Factors Influencing Soil Classification Using Normalized Piezocone Tip Resistance and Pore Pressure Parameters", Journal Geotechnical and Geoenvironmental Engineering, 134 (11), 1569-1586.

Seed H. B., Tokimatsu K., Harder, L. F., Chung R. M., (1984), "The Influence of SPT procedures in soil liquefaction resistance evaluations", Technical Report No: UCB/EERC-84/15, Earthquake Engineering Research Center, University of California, USA.

Sivrikaya O., Toğrol E., (2003), "İnce daneli zeminlerde SPT sonuçlarının düzeltilmesi üzerine bir çalışma", İTÜ Dergisi Seri D: Mühendislik, 2(6), 59 - 67.

Tarı U., Tüysüz O., (2016), “The effects of the North Anatolian Fault on the geomorphology in the Eastern Marmara Region, Northwestern Turkey”, *Geodinamica Acta*, 28(3), 139-159.

Ulusay R., (2010), “Uygulamalı Jeoteknik Bilgiler”, 5th Edition, TMMOB Jeoloji Mühendisleri Odası Yayınları.

Vlasblom A., (1985), “The Electrical Penetrometer: A Historical Account of Its Development”, *Delft Soil Mechanics Laboratory*, 92, 51.

Web 1, (2021), <http://www.kuzeymarmaraotoyolu.com>, (Erişim Tarihi: 22/05/2021).

Web 2, (2022), <https://gouda-geo.com/product/piezocones-and-electric-cpt-cones>, (Erişim Tarihi: 17/05/2022).

Web 3, (2022), <https://cdnsiencepub.com/doi/10.1139/cgj-2012-0278?mobileUi=0>, (Erişim Tarihi: 17/05/2022).

Web 4, (2022), [https://tr.wikipedia.org/wiki/Sakarya\\_Nehri](https://tr.wikipedia.org/wiki/Sakarya_Nehri), (Erişim Tarihi: 17/05/2022).

Wissa A. F. Z., Martin R. T., Garlanger J. E., (1975), "The Piezometer Probe", *American Society of Civil Engineers Specialty Conference on In Situ Measurement of Soil Properties*, 536-545, North Carolina, USA, 1-4 June.

Zhao X., Cai G., (2015), “SPT–CPT Correlation and Its Application for Liquefaction Evaluation in China”, *Marine Georesource Geotechnology*, 33(3), 272–281.

## **BIOGRAPHY**

Mustafa HABİBOĞLU successfully completed the Civil Engineering Department of Yeditepe University Engineering Faculty, which he started in 2014, in 2019. He worked as a Civil Engineer in the Mediterranean-Black Sea Road project while he was studying at the Gebze Technical University.



# APPENDICES

## Other Appendices (CD)

